A late Pleistocene-Holocene multi-proxy record of palaeoenvironmental change from Still Bay, southern Cape coast, South Africa

Lynne J. Quick[1*], Andrew S. Carr[2], Michael E. Meadows[1], Arnoud Boom[2], Mark D. Bateman[3], David L Roberts[4], Paula J. Reimer[5], Brian M. Chase[6]

[1]Department of Environmental and Geographical Science, University of Cape Town, Private Bag X3, Rondebosch 7701, South Africa.

[2]Department of Geography, University of Leicester, Leicester, LE1 7RH, United Kingdom.

[3]Department of Geography, University of Sheffield, Sheffield, S102TN, United Kingdom.

[4]Geography Department, University of the Free State, P.O. Box 339, Bloemfontein 3900, South Africa.

[5]School of Geography, Archaeology and Palaeoecology, Queen's University Belfast, Belfast, BT7 1NN, Northern Ireland, UK.

[6]Centre National de Recherche Scientifique, UMR 5554, Institut des Sciences de l'Evolution de Montpellier, Département Environnements, Université Montpellier 2, Bat.22, CC061, Place Eugène Bataillon, 34095 Montpellier, cedex 5, France.

Corresponding author: Lynne J. Quick, email: lynne.j.quick@gmail.com

The southern Cape is a key focus for southern African palaeoenvironmental research as it represents the transitional region between temperate westerlies and sub-tropical rainfall sources. This study presents pollen, plant biomarker, geochemical and charcoal data preserved in the Rietvlei wetland. The bulk of the record spans the last 16 kyr, but it also provides rare insights into late MIS 3 (c. 35-30k cal a BP). The data suggest that during the Pleistocene the development and permanence of this wetland was likely influenced by sea-level change via control on the local water table; notably lower sea levels within MIS 2 resulted in very limited wetland productivity. The MIS 3 section provides evidence both supporting previous suggestions of relatively humid conditions, but also some indication of periodic arid phases. The Holocene record suggests clear contrasts between the early (11-7k cal a BP – relatively humid), mid-Holocene (7-3.3k cal a BP; more arid, less productive wetland conditions) and latest Holocene (last 2k cal a BP resurgence in both fynbos and aquatic/riparian pollen). While isolating the roles of winter/summer rainfall remains challenging, these data clarify the nature of change during key episodes in the regional palaeoenvironmental record.

Keywords: late Pleistocene, Holocene, multi-proxy record, southern Cape palaeoenvironments, South Africa

1 INTRODUCTION

The southern Cape coast of South Africa currently encompasses the transition between 1) the southern African winter rainfall zone in the west, which receives most of its precipitation from seasonal migrations of the southern westerlies, and 2) the summer rainfall zone in the east, where moisture is primarily advected from the Indian Ocean during the summer (Chase and Meadows, 2007; Figure 1). As a result, it receives precipitation from multiple potential sources, and much of the region presently experiences a largely aseasonal rainfall regime. However, as the influence of both winter and summer moisture-bearing systems was highly variable during the late Quaternary (Talma and Vogel, 1992; Parkington et al., 2000; Truc et al., 2013; Chase et al., 2015), the southern Cape has been identified as being a particularly sensitive climatic region, with potentially radical changes in rainfall seasonality and amount (Chase and Meadows, 2007). Such sensitivity (and complexity) is also compounded by the dynamics and interactions associated with the adjacent warm Indian Ocean Agulhas Current, the Subtropical Front (STF) and the cold southeast Atlantic Benguela Current. Variability in these systems is known to influence local terrestrial climate (Cohen and Tyson, 1995; Chase et al., 2013; Chase et al., 2015) and each are important components modulating global thermohaline circulation (Peeters et al., 2004; Bard and Rickaby, 2009; Caley et al., 2011a).

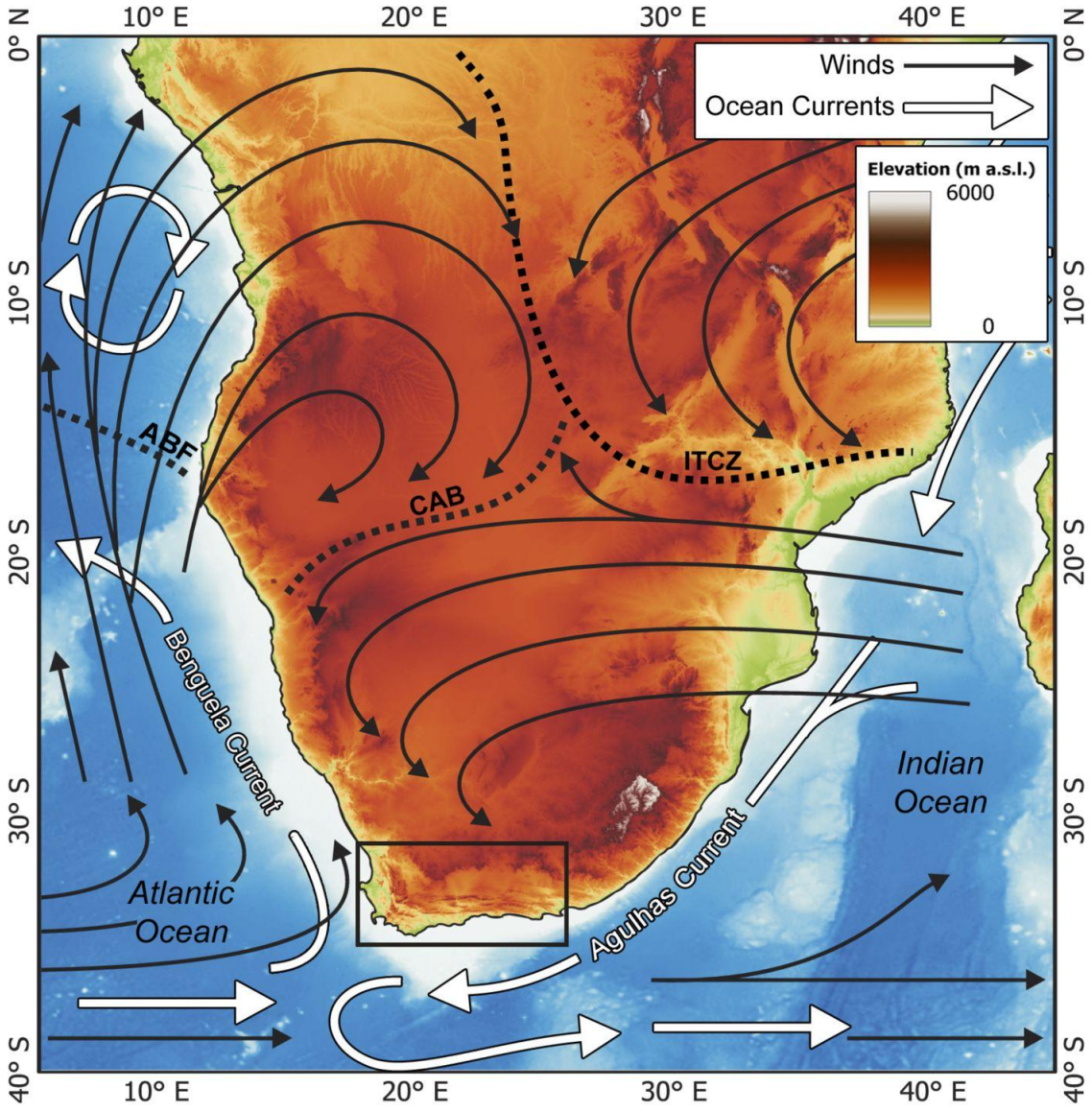

Figure 1 *The location of the southern Cape (black box) in relation to generalised atmospheric and oceanic circulation patterns. ABF: Angola-Benguela Front, CAB: Congo Air Boundary, ITCZ: Inter Tropical Convergence Zone.*

The southern Cape coastal lowlands include a significant portion of the Fynbos Biome - the dominant vegetation of the Cape Floristic Region, which is known for its exceptionally high levels of species richness and endemism, elements of the Albany Thicket Biome and rare afrotemperate forest patches (Mucina and Rutherford, 2006; Figure 2). Despite their botanical significance and high conservation status, there is almost no palaeoenvironmental/ecological data pertaining to the history of these coastal lowlands. Most published data comprise fragmentary records (e.g. Martin, 1968; Scholtz, 1986; Carr et al.,

2006b), often not extending beyond the Holocene, and a coherent history of long-term environmental/ecological change remains to be established.

Here we report the palaeoenvironmental records preserved in the Rietvlei wetland near to Still Bay on the Riversdale Plain (Figure 2). Through the analysis of sediments from a core extracted at this site, we investigate the relationship between changing rainfall seasonality and vegetation dynamics, including the responses of particular vegetation types (fynbos and non-fynbos communities) to late Quaternary environmental change.

An initial study of the Rietvlei-Still Bay site (Carr et al., 2010) demonstrated the preservation of a record encompassing the last 37 kyr. That study focused on the site's organic geochemical record (using pyrolysis-gas chromatography/mass spectrometry; py-GC/MS), and changing organic matter (OM) preservation and provenance. The present study (based on the same core as the initial study by Carr et al., 2010) seeks to build on this through the development of a more detailed site chronology and new lines of proxy evidence, including pollen and microscopic charcoal, as well as an expanded stable isotope and plant leaf wax lipid dataset. The specific objectives are to characterise the local wetland conditions at Rietvlei-Still Bay and to reveal palaeovegetation and associated palaeoclimatological evidence that offers new insights into the nature of climate and ecological change along the southern Cape coast during the late Pleistocene and Holocene.

2 STUDY REGION AND SITE DESCRIPTION

2.1 Location, geology, geomorphology and climate

The sediment core analysed for this study was extracted from Rietvlei (34° 21.249'S; 21° 32.127'E, 17 m a.s.l.), an elongated wetland (approximately 3.5 km long and 100 m wide) situated on the Riversdale Plain about 8 km east of the town of Still Bay and ~300 km east of Cape Town (Figure 2). The wetland occupies a distinct topographic depression between two shore-parallel coastal barrier dunes and probably originated as an inter-dunal slack lake (Roberts et al., 2008). The landwards barrier comprises well-cemented aeolianite of the Waenhuiskrans Formation, which was likely established within MIS 7 whereas the seawards barrier was formed during and subsequent to the Last Interglacial sea level high stand (MIS 5e; ~125ka) (Roberts et al., 2008). The area is underlain by Bokkeveld Group mudrocks (part of the Cape Supergroup). Up to 8 m of sediment has accumulated within Rietvlei, a substantial proportion of which comprises alluvial (calcareous) silty sands. The upper 3 m of

sediment contains significant amounts of organic matter. Today the waters of the wetland are moderately alkaline and are covered with a floating mat of vegetation, dominated by *Phragmites australis*.

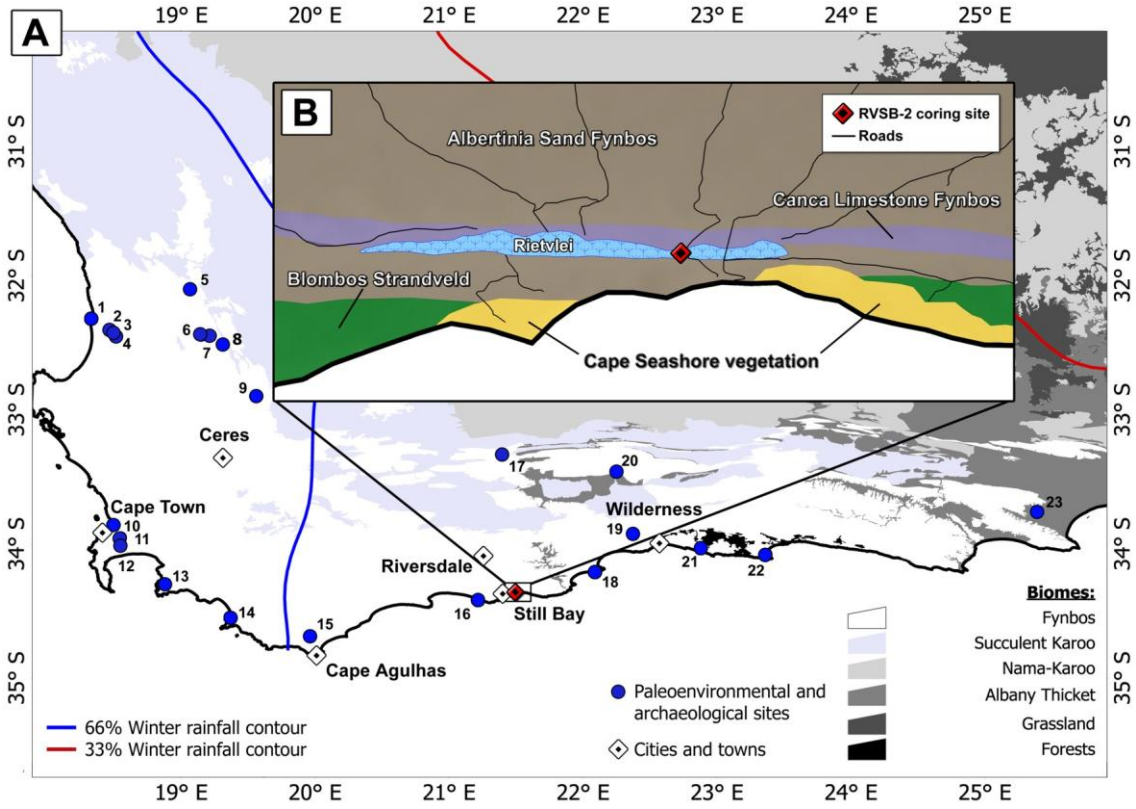

Figure 2 *A map showing the location of the Rietvlei wetland, the approximate positions of the winter rainfall (WRZ), year-round rainfall (YRZ) and summer rainfall (SRZ) zones, the biomes of South Africa (Mucina and Rutherford, 2006) and the published palaeoenvironmental and archaeological records within the region (A). 1 Elands Bay Cave, 2 Grootdrift, 3 Verlorenvlei, 4 Klaarfontein Springs, 5 Pakhuis Pass, 6 Sneeuberg Vlei and Driehoek Vlei, 7 De Rif, 8 Truitjes Kraal, 9 Katbakkies, 10 Rietvlei, 11 Cape Flats, 12 Princess Vlei, 13 Hangklip, 14 Die Kelders, 15 The Agulhas Plain vleis and lunettes (Soetendalsvlei, Voëlvlei, Renosterkop and Soutpan), 16 Blombos Cave, 17 Seweweekspoort 18 Pinnacle Point, 19 Norga peats, 20 Cango Cave and Boomplaas Cave, 21 Groenvlei, 22 Nelson Bay Cave and 23 Uitenhage Aquifer. The position of the coring site (RVSB-2) in relation to the wetland and local vegetation (Mucina and Rutherford, 2006) (B).*

Precipitation at the site averages ~400 mm (Climate Systems Analysis Group, 2012) and the climate is classified as semi-arid. Situated in the year-round rainfall zone (YRZ; sensu Chase and Meadows, 2007; Figure 1), precipitation is distributed in a relatively

uniform pattern throughout the year. During the winter months, the expansion of the circumpolar vortex drives the equatorward migration of the westerly storm track, while in the summer months, warmer sea-surface temperatures and increased easterly flow result in precipitation events. It has been suggested that as a function of changes in global glacial-interglacial boundary conditions reductions, or even cessations, in the contributions of these moisture-bearing systems may have occurred, resulting in shifts between a year-round, summer or winter rainfall climate (Chase and Meadows, 2007). This may have meant the potential development of a pronounced drought season, which currently exists to the west in the purely winter-rainfall Western Cape.

2.2 Contemporary vegetation

The aeolianite ridge north of Rietvlei is dominated by endemic-rich limestone fynbos (Mustart et al., 2003; Figure 2). The distribution of limestone fynbos is largely controlled by edaphic factors and it is only found on the alkaline soils of the Bredasdorp Group limestones and aeolianites. Due to its highly specialised and restricted nature, it represents one of the most threatened fynbos vegetation types (Cowling and Holmes, 1992; Willis et al., 1996). Structurally, limestone fynbos is dominated by asteraceous, restioid and proteoid fynbos with graminoid and ericaceous fynbos largely absent (Mucina and Rutherford, 2006). Sand fynbos borders the patches of limestone fynbos (Figure 2), and is more extensive than the limestone fynbos, being concentrated within valleys and on the coastal plain. It is structurally defined as proteoid fynbos and characterised by medium to tall open shrublands (Mucina and Rutherford, 2006). To the south of the site, the coastal dune crests and their landward slopes are vegetated by coastal thicket (‘strandveld’), comprising a high cover of tall non-proteoid trees and shrubs (e.g. *Sideroxylon inerme* and various trees of the Celastraceae family) and a high presence of fleshy-leaved shrubs (e.g. *Zygophyllum morgsana*) (Rebelo et al., 1991; Mustart et al., 2003). This vegetation type is characterised by the co-dominance of *Euclea racemosa* and *Olea exasperata*. The thicket elements form a mosaic with dune asteraceous fynbos on the neutral sands to the south west and south east of the site (Rebelo et al., 1991; Mucina and Rutherford, 2006; Figure 2). The wetland itself is extensively covered by *Phragmites australis*. Also within the floating mat of emergent vegetation are various Juncaceae, Cyperaceae, Apiaceae and Araceae species, as well as true aquatic elements such as *Aponogeton* sp.

3 MATERIALS AND METHODS

3.1 Core extraction

An undisturbed continuous sediment sequence was extracted with a portable vibracorer (adapted from Lanesky et al., 1979; detailed methodology found in Baxter, 1996). Two field excursions to Rietvlei in 2007 and 2009 yielded three cores. All three cores revealed comparable stratigraphies, Rietvlei-Still Bay 2 (RVSB-2) was assessed as having the greatest potential for the generation of a multi-proxy palaeoenvironmental record and is therefore the focus of this study. After retrieval, RVSB-2 was split in the laboratory, initially under darkroom conditions to allow sampling for optically stimulated luminescence (OSL) dating. Following this, sequential sub-sampling took place along the length of the core for radiocarbon, pollen and charcoal (combined within one sample), sedimentological, and various geochemical analyses.

3.2 Chronology

The RVSB-2 age model was constructed from a combination of radiocarbon and OSL ages (Table 1). Initially, four radiocarbon ages were obtained from the Department of Geosciences, University of Arizona using gas proportional counting (GPC). Samples were pre-treated with hydrochloric acid (HCl) and sodium hydroxide (NaOH) (to remove any alkali-soluble organic carbon) and rinsed with dilute HCl. Samples were combusted in oxygen to produce CO_2 and purified. Four AMS (accelerator mass spectrometry) radiocarbon samples were subsequently taken from positions in the core related to significant changes in organic matter composition and provenance (see Carr et al., 2010). The AMS samples were processed at the ^{14}CHRONO Centre, Queen's University Belfast. These samples were treated with HCl (4%), and heated to 80°C for 2–3 hours. This was followed by NaOH treatment (2%, at 80°C for 2 hours) to remove humic acids and further HCl (2%) pre-treatment for one hour at room temperature. The radiocarbon ages were calculated using the Libby half-life of 5568 years following Stuiver and Polach (1977). The ages were corrected for isotope fractionation using the AMS-measured δ^{13}C, which accounts for both natural and machine fractionation.

The radiocarbon chronology was augmented with an OSL sample (Shfd08157) from 224.5 cm. The OSL age was obtained on extracted and cleaned coarse grained (180-250 μm) quartz with a palaeodose (De) measured using the single aliquot regeneration protocol (further details are provided in Bateman and Catt (1996) and Roberts et al. (2008)). A De of 7.1 ± 0.09 Gy was obtained from 24 measured replicates which were normally distributed

with a low over dispersion (OD = 7%). Dose rates were derived from elemental concentrations obtained from inductively-coupled mass spectrometry suitably attenuated for sediment size and moisture content. The latter were based on the contemporary (measured) content of the sub-sample with an uncertainty of 5% to account for potential changes in wetland conditions. As the sand rich layer sampled for OSL was thin, dose rates were measured for adjacent units and the gamma contribution from these units factored in to the final dose rate using gamma gradients as reported in Aitken (1985). The cosmic dose contribution was derived from the equation of Prescott and Hutton (1994). The final calculated dose-rate for sample Shfd08157 was 0.63 ± 0.027 Gy/ka.

The software package *Bacon* (version 2.2) (Blaauw and Christen, 2011) was used to integrate the chronological information and to develop an age-depth model (Figure 3). Using a Bayesian statistics framework, this method divides the core into sections and models the accumulation rate for each section through multiple Markov Chain Monte Carlo (MCMC) iterations. ^{14}C ages were calibrated with the SHCal13 curve (Hogg et al., 2013) and the post-bomb age was calibrated with the Southern Hemisphere post-bomb curve by Hua et al. (2013). The OSL age with its uncertainties was incorporated into the age-depth model as a 'calibrated' age.

3.3 Bulk sample organic matter content

Bulk geochemical analyses comprising total organic carbon (TOC), total nitrogen (TN) and $\delta^{13}C_{TOC}$ were carried out using a SerCon ANCA GSL elemental analyser interfaced to a SerCon Hydra 20–20 continuous flow isotope ratio mass spectrometer. For the determination of the TOC and $\delta^{13}C_{TOC}$, samples were pre-treated with 10% HCl to exclude inorganic carbon. All analyses were carried out in triplicate with a typical precision of ~0.05% for elemental concentrations and 0.1‰ for $\delta^{13}C_{TOC}$.

3.4 Pollen analysis

For pollen and microscopic charcoal analyses, the sub-sampling interval was guided by stratigraphic complexity. An initially coarse sampling resolution (~10 cm), was refined (~1 to 5 cm) to better characterise what were identified as periods of significant vegetation change.

The extraction of palynomorphs followed standard methods for the removal, disintegration and dissolution of the non-pollen matrix (Moore et al., 1991) with specific adaptations for dense media separation from Nakagawa et al. (1998). This involved 30% HCl treatment to remove carbonates, 10% KOH digestion to disaggregate the samples and remove humic acids, heavy liquid mineral separation using $ZnCl_2$ to separate the pollen grains from

the mineral fraction (Faegri and Iversen, 1989; Moore et al., 1991; Nakagawa et al., 1998) and for samples with high clay content, HF treatment to remove remaining siliceous material. Samples were acetolysised and mounted in *Aquatex* (aqueous mounting agent). Three slides were produced per sample. To determine absolute pollen concentrations *Lycopodium* spores were added (Stockmarr, 1973) prior to physical and chemical processing to ensure even losses amongst fossil and exotic grains during processing.

Pollen counts of 500 grains per sample were carried out at 400x magnification for routine identification and 1000x for specific identification. Spores and other non-pollen palynomorphs were also counted, but not included in the total pollen sum. Pollen taxa were identified using the University of Cape Town's reference collection and published literature (van Zinderen Bakker, 1953, 1956; van Zinderen Bakker and Coetzee, 1959; Welman and Kuhn, 1970; Scott, 1982). The pollen and microscopic charcoal diagrams were divided into statistically significant pollen assemblage zones based on a CONISS (Constrained Incremental Sum of Squares) (with square root transformation) analysis (Grimm, 1987).

3.5 Microscopic charcoal analysis

Charcoal particles were identified and counted on the same microscope slides produced for the pollen analysis. Only particles that were black, opaque and angular were considered charcoal fragments (Patterson et al., 1987; Mooney and Tinner, 2011). Charcoal fragments were classified and counted according to two size groups based on the long axis of each fragment; 10 – 100 µm and 100 – 150 µm. Particles less than 75 μm^2 (or ~ 10 µm long) were not counted due to the risk of false identification (Mooney and Tinner, 2011). Therefore our charcoal signal primarily relates to the regional (10 – 100 µm) and local (100 – 150 µm) fire signals and excludes extra-regional fires (<10 µm). Absolute charcoal abundances were calculated in the same manner as pollen concentrations (Stockmarr, 1973).

3.6 Leaf wax lipids

In South Africa recent studies have shown that the relative abundances of leaf wax *n*-alkanes may be an environmentally sensitive parameter (Carr et al., 2014; 2015). Additionally, the relative abundance of short and long chain length n-alkanes in lacustrine and wetland contexts shifts have been associated with changes in the contribution of aquatic and riparian plant types to sedimentary organic matter (e.g. Ficken et al., 2000). Here we present data for leaf wax *n*-alkane distributions for the Rietvlei sediments. Leaf wax lipids were extracted from 5-10 g of powdered sediment using a soxhlet extraction system (24 hours: hexane, DCM and methanol; ratio 1:2:2). The extracts were rotary evaporated and purified over a

sodium sulphate column. The apolar fraction was isolated via Al_2O_3 column chromatography using a hexane/DCM mixture (9:1). Gas chromatography was carried out on a Perkin Elmer Clarus 500 GC/MS equipped with a CP-Sil 5CB (30 m x 0.25 mm) column. The GC oven programme comprised an initial temperature of 60°C, ramped to 120°C at 20°C min^{-1}, increased to 325°C at 4°C min^{-1} and held for 15 minutes. Compounds were identified on the basis of mass spectra and retention times. *n*-alkane retention times were confirmed with an authenticated standard. The following indices were used to characterise the resulting *n*-alkane leaf wax distributions:

The Carbon Preference Index (CPI) is a measure of the odd chain length verses even number chain length dominance. It is primarily used to confirm the origin of the extracted *n*-alkanes as being derived from plant leaf waxes and as a check for hydrocarbon / petroleum contamination (which typically have no odd/even chain length dominance; CPI = 1). CPI was calculated following Bray and Evans (1961).

$$CPI_{25\text{-}33} = \frac{1}{2}\left(\frac{C25+C27+C29+C31+C33}{C24+C26+C28+C30+C32}\right) + \left(\frac{C25+C27+C29+C31+C33}{C26+C28+C30+C32+C34}\right) \quad (1)$$

Where C_x is the concentration of the *n*-alkane with x carbon atoms.

The average chain length (ACL) was calculated as per equation 2, which is equivalent to the weighted mean of all odd chain length *n*-alkanes, following Poynter et al., (1989).

$$ACL_{23\text{-}33} = \frac{23*C23+25*C25+27*C27+29*C29+31*C31+33*C33}{C23+C25+C27+C29+C31+C33} \quad (2)$$

Where C_x is the concentration of the *n*-alkane with x carbon atoms.

A ratio of shorter to longer chain length *n*-alkanes (the P_{aq} index) has been used to differentiate aquatic and emergent vegetation inputs. Such an approach was initially based on measurements of modern emergent and aquatic plants in East African lakes. It is calculated following Ficken et al (2000):

$$P_{aq} = \frac{(C23+C25)}{(C23+C25+C29+C31)} \quad (3)$$

Where C_x is the concentration of the *n*-alkane with x carbon atoms. A higher P_{aq} is associated with a greater proportion of shorter chain length *n*-alkanes and therefore larger contributions of emergent or aquatic vegetation relative to terrestrial vegetation.

3.7 Pyrolysis-Gas chromatography mass spectrometry

Py-GC/MS analyses can be used to characterise complex (insoluble) macromolecular organic matter (Nierop, 1998; Kaal et al., 2007). The technique thermally fragments this macromolecular material into GC-amenable products and the resulting pyrolysis products are interpreted in terms of their probable precursor macromolecules (e.g. lignin monomers and cellulose) which are potentially diagnostic of OM provenance and/or preservation (e.g. Vancampenhout et al., 2008; Carr et al., 2013). Carr et al. (2010) presented a suite of py-GC/MS data for 22 samples from the RVSB2 core. These demonstrated marked down core changes in OM composition, and were inferred to reflect the combined effects of changing organic matter preservation and changes in organic matter provenance (particularly the presence of algal lipids). Here, these effects were inferred using axes one and two from a de-trended correspondence analysis (DCA, conducted in *Past* (Hammer et al., 2001)) of the complete py-GC/MS dataset from Rietvlei. Here we include the axis 1 (OM preservation) and 2 (OM source) scores, now integrated with the site's improved age-depth model as an additional proxy data source. Methodological information and further details are provided in Carr et al. (2010).

4 RESULTS

4.1 Stratigraphy and chronology

The 360 cm core consists primarily of poorly-sorted silty sands with slightly higher clay and silt fractions at 130 cm and from 280 cm to 325 cm (Figure 3). The 280 – 325 cm section is distinct from the rest of the sequence comprising of pale carbonate-rich marls with feint orange mottles. The top 70 cm of the core contains abundant macro-plant remains predominantly of *Phragmites australis*. Mollusc shells and fragments of other marine micro-fauna were found throughout most of the core and are especially prevalent between 150 and 280 cm. These are most likely derived from the aeolianite and active coastal dunes that flank the site.

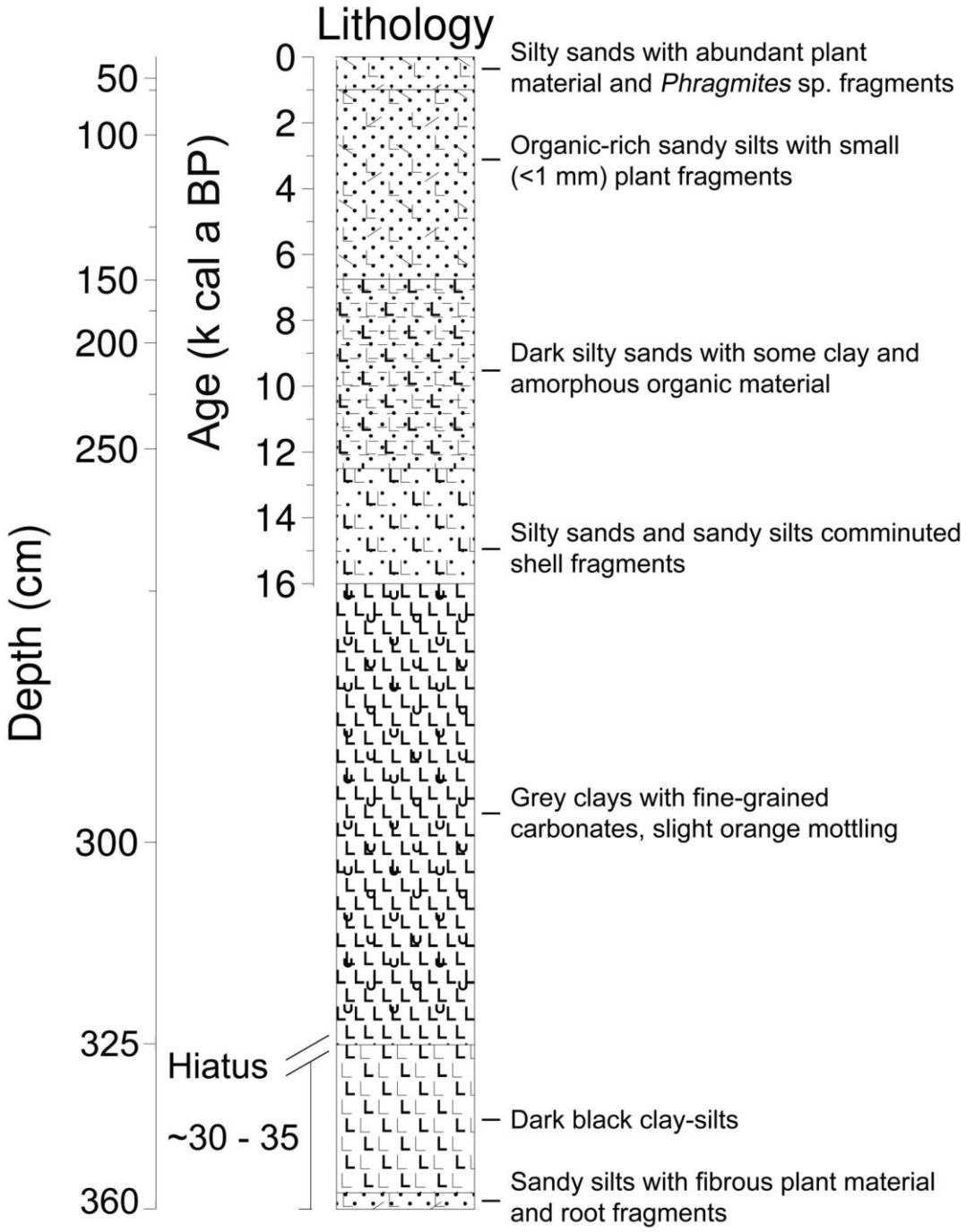

Figure 3 *Stratigraphic description of the RVSB-2 core employing the Troel-Smith sediment notation.*

The bulk of RVSB-2 record spans the last 16k cal a BP (Table 1; Figure 4) including the terminal glacial period (~16 – 11.7k cal a BP) and the Holocene (11.7k cal a BP to present).

Orange mottles evident between 280 cm (~16k cal a BP) and 325 cm represent minor oxidation that could be a result of shallow-water conditions in the wetland or sub-aerial exposure of the sediment during that period (Carr et al., 2010). It is not possible to establish a reliable chronology for this unit. At 325 cm, an abrupt contact between the grey, carbonate clays and the underlying organic-rich sediments indicates a likely hiatus in the sequence. The two radiocarbon ages from the basal peat, while inverted and measured with different techniques, are within errors of one another. We do not apply an age-depth model to this unit, but consider the proxy data as a snapshot of environmental conditions ~30 – 35k cal a BP.

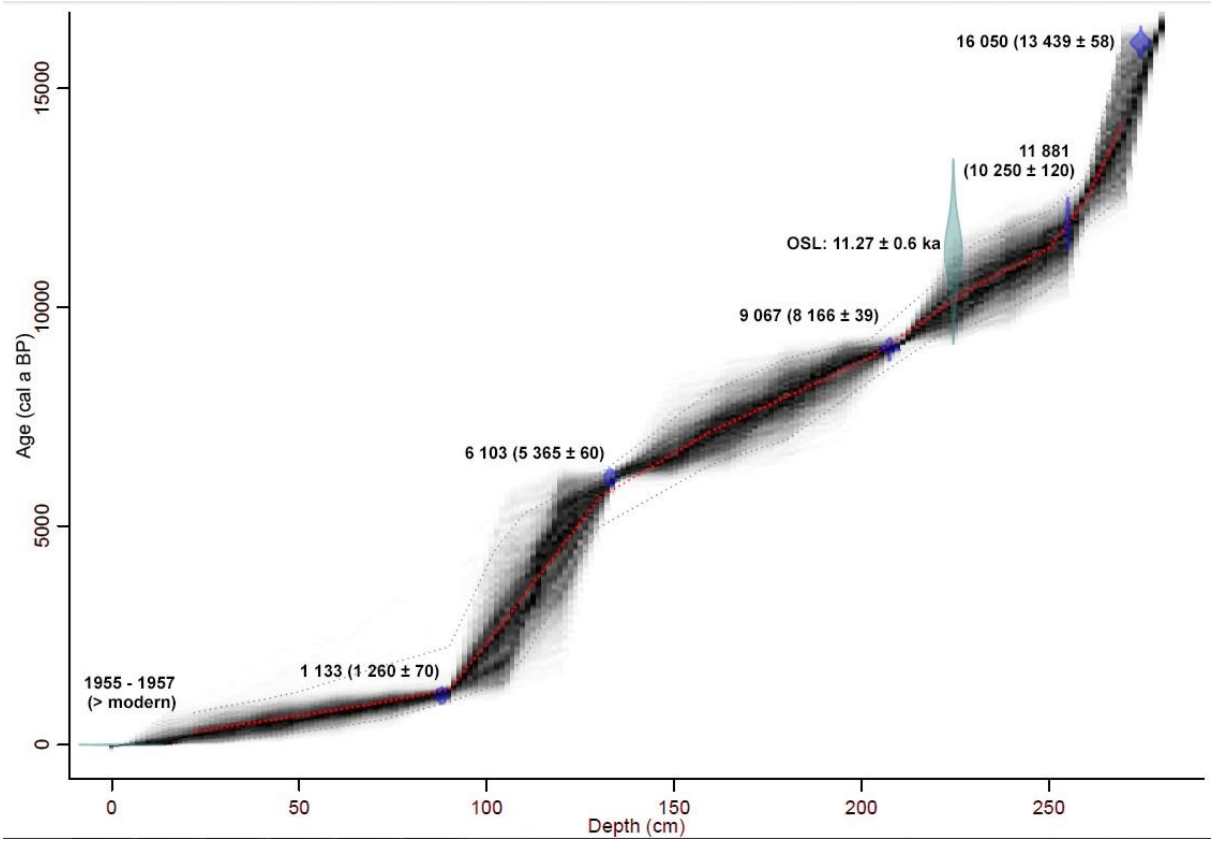

Figure 4 *The RVSB-2 age-depth model produced by the Bacon software package (Blaauw and Christen, 2011).* ^{14}*C ages were calibrated with the SHCal13 curve (Hogg, 2013) and the post-bomb age was calibrated with the Southern Hemisphere post-bomb curve by Hua et al. (2013). The median probability calibrated ages are labelled and the uncalibrated ages with errors are provided in parentheses (apart from the first age range which is the greater than modern sample's AD date range). The model is based on 19 15-cm thick sections of piece-wise linear accumulations, grey-scales indicate all likely age-depth models, grey dotted lines show the 95% confidence intervals and red curve shows single 'best' model based on the*

weighted mean age for each depth. Note the OSL date is not calibrated nor reported BP but for ease of plotting has been included on the same axis label.

4.2 Pollen and microscopic charcoal analyses

A total of 86 samples were processed for pollen and microscopic charcoal analysis. Pollen preservation was variable, with relatively high pollen concentrations (mean = 7.2×10^4 grains g^{-1}) within the top two metres of the core, below which concentrations dropped considerably towards the base. Two sections of the core, from 220 – 260 cm and 290 – 325 cm (corresponding to the base of a sand layer and the calcareous/clay-rich zone (Figure 3)), were either devoid of pollen or contained excessively low concentrations.

Figure 5 *Relative percentage pollen diagram for RVSB-2. Taxa are grouped according to general ecological affinities and are plotted against interpolated age (k cal a BP). Exaggeration curves are 5x and taxa representing less than 1% for any given level are presented as presence points. Non-pollen palynomorphs are represented as percentages of the total pollen count but not included in the count. Zonation is based on the results of a CONISS analysis.*

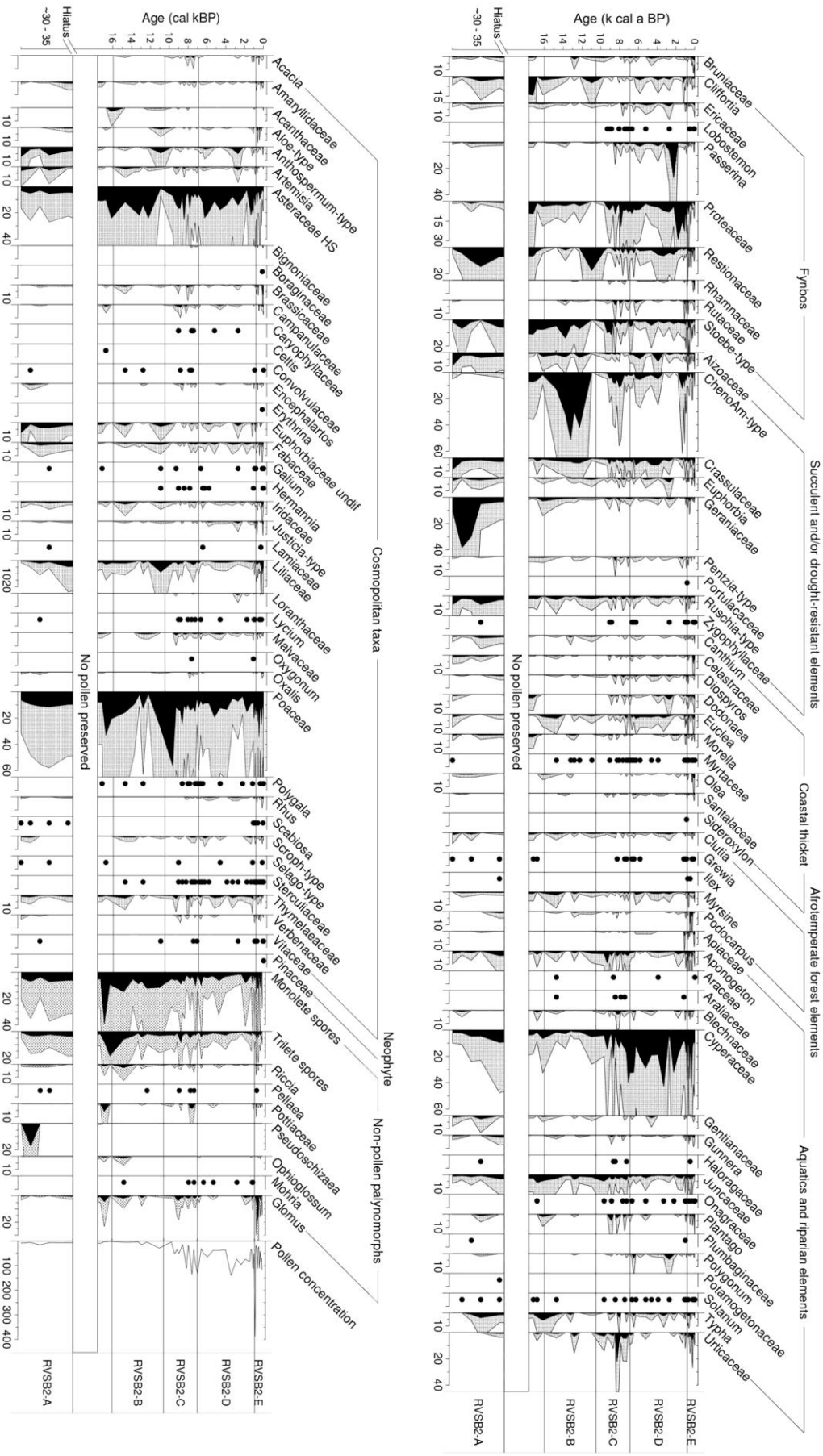
Age (k cal a BP)
Hiatus
~30 - 35
Bruniaceae
Cliffortia
Ericaceae
Lobostemon
Passerina
Proteaceae
Restionaceae
Rhamnaceae
Rutaceae
Stoebe-type
Aizoaceae
ChenoAm-type
Crassulaceae
Euphorbia
Geraniaceae
Pentzia-type
Portulacaceae
Ruschia-type
Zygophyllaceae
Canthium
Celastraceae
Diospyros
Dodonaea
Eucnea
Morella
Myrtaceae
Olea
Santalaceae
Sideroxylon
Clutia
Grewia
Ilex
Myrsine
Podocarpus
Apiaceae
Aponogeton
Araceae
Araliaceae
Blechnaceae
Cyperaceae
Gentianaceae
Gunnera
Haloragaceae
Juncaceae
Onagraceae
Plantago
Plumbaginaceae
Polygonum
Potamogetonaceae
Solanum
Typha
Urticaceae
No pollen preserved
Fynbos
Succulent and/or drought-resistant elements
Coastal thicket
Afrotemperate forest elements
Aquatics and riparian elements
RVSB2-A
RVSB2-B
RVSB2-C
RVSB2-D
RVSB2-E
Age (cal kBP)
Acacia
Amaryllidaceae
Acanthaceae
Aloe-type
Anthospermum-type
Artemisia
Asteraceae HS
Bignoniaceae
Boraginaceae
Brassicaceae
Campanulaceae
Caryophyllaceae
Celtis
Convolvulaceae
Encephalartos
Erythrina
Euphorbiaceae undif
Fabaceae
Galium
Hermannia
Iridaceae
Justicia-type
Lamiaceae
Liliaceae
Loranthaceae
Lycium
Malvaceae
Oxygonum
Oxalis
Poaceae
Polygala
Rhus
Scabiosa
Scroph-type
Selago-type
Sterculiaceae
Thymelaeaceae
Verbenaceae
Vitaceae
Pinaceae
Monolete spores
Trilete spores
Riccia
Pellaea
Pteridaceae
Pseudoschizaea
Ophioglossum
Mohria
Glomus
Pollen concentration
x10³
Cosmopolitan taxa
Neophyte
Non-pollen palynomorphs

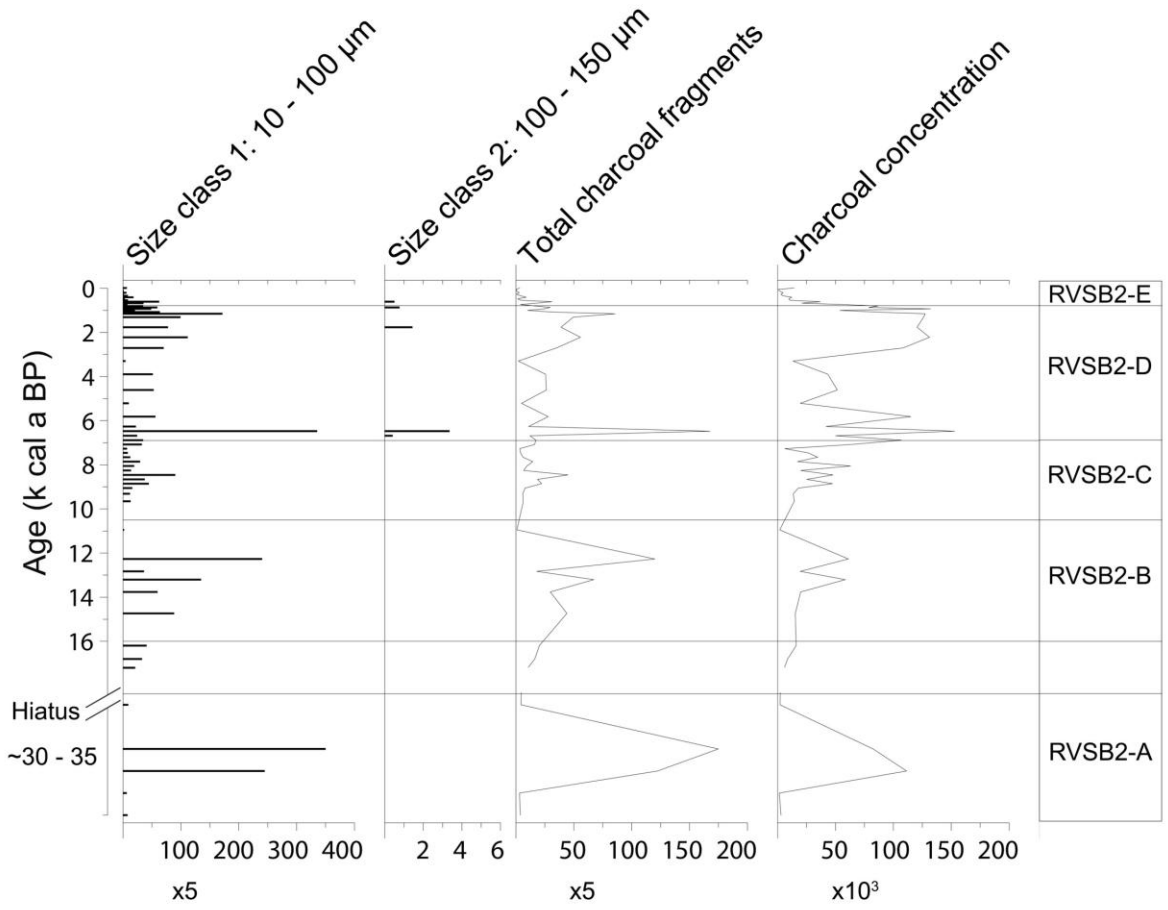

Figure 6 *Microscopic charcoal fragments per gram sample in the RVSB-2 core, illustrated for the two size classes and the total fragments. Charcoal concentration calculated in the same manner as pollen concentrations using Lycopodium spore counts. The zonation is based on the pollen record.*

Five pollen zones were identified (on the basis of the CONISS analysis). The most distinctive features of the lowermost pollen assemblage zone (RVSB2-A; ~35 – 30k cal a BP, the basal unit) is the high microscopic charcoal amounts and concentrations and the high percentages of Geraniaceae pollen (Figure 5 and 6). There are relatively elevated proportions of Aizoaceae, Crassulaceae, *Ruschia*-type, *Euphorbia*, *Artemisia* and *Anthospermum*-type pollen in comparison to the rest of the sequence. Local wetland taxa percentages (particularly Cyperaceae and Juncaceae) are low. Above the marls (representing c.30-16k cal a BP, and lacking preserved pollen), pollen zone RVSB2-B (~16 – 11k cal a BP) is characterised by an abundance of Asteraceae, *Stoebe*-type and *ChenoAm*-type. The latter reaches exceptionally high percentages (30 – 50%) between 13.8 – 12.3k cal a BP coinciding with increased charcoal concentrations and relatively low percentages of aquatic/riparian pollen.

The oldest section of zone RVSB2-C (total age range ~11 – 7k cal a BP) comprises only two levels with sufficient pollen for analysis at 11k cal a BP and 9.7k cal a BP. These samples are characterised by extremely high percentages of Poaceae pollen. After 9.7k cal a BP, pollen concentrations increase significantly. Proteaceae percentages increase from 9.3k cal a BP until the top of RVSB2-C, *Stoebe*-type proportions are elevated from 9.3k cal a BP to 8.9k cal a BP and Asteraceae peaks from 9.3 – 8.5k cal a BP before tapering towards the top of the zone. A similar trend is evident for charcoal amounts and concentrations. Local aquatic and riparian taxa percentages, notably Cyperaceae and *Aponogeton* are relatively high from 9.3k cal a BP to the top of RVSB2-C. Cyperaceae generally increases towards the top of RVSB2-C, reaching a maximum of nearly 40%, and from this point until the late Holocene remains the dominant pollen type.

The most distinguishing features of zone RVSB2-D (~7.0 – 0.8k cal a BP) are prominent peaks in *Passerina* (27%) at 2.6k cal a BP and Proteaceae (29%) pollen at 2k cal a BP and the continued high percentages of Cyperaceae throughout the zone. Proteaceae percentages (together with many other fynbos elements) are relatively low for the lower half of the zone (from 7.0 – 2.6k cal a BP) increasing to 10 – 30% at the top (from 2.2 – 0.8k cal a BP). *Dodonaea* reaches its highest percentage at 2.7k cal a BP. Other coastal thicket taxa are slightly elevated (e.g. *Euclea*) in comparison to previous zones. Among the afrotemperate elements, *Grewia* is absent for much of this pollen zone. There are discrete peaks in Aizoaceae and Crassulaceae at 3.9k cal a BP. Charcoal concentrations are high near the base and at the top of RVSB2-D. Among the aquatic and riparian pollen types RVSB2-D shows a reduction in the abundance of Juncaceae, *Aponogeton* and Urticaceae. Total charcoal amounts generally increase towards the top of RVSB2-D however there are discrete peaks in both size classes near the base of the zone (at 6.5k cal a BP).

The uppermost pollen zone (RVSB2-E; ~0.8 – 0k cal a BP) is primarily defined by the greater proportions of coastal thicket taxa (e.g. Celastraceae, *Dodonaea*, *Euclea* and *Olea*). There is an increase in local wetland taxa with significant peaks in *Aponogeton*, *Plantago* and Cyperaceae. Charcoal amounts and concentrations are generally low within zone RVSB2-E, while pollen concentrations are extremely high (reaching $3.9x10^5$ grains g^{-1} at the base of RVSB2-E).

4.3 Bulk-sample geochemistry

The bulk geochemical variables (TOC, TN, TOC/TN, Figure 7) correlate well with pollen concentrations and indicate that the degree of pollen preservation is closely associated with

the depositional environment. The py-GC/MS data (specifically DCA axis 1; Figure 7) similarly demonstrate very varied organic matter preservation and this parameter closely tracks TOC (Carr et al. 2010), which varies down-core from 0.5 to 30%. In general, TOC is highest within the top 200 cm of the core (~8.5k cal a BP), with particularly high values associated with pollen assemblage zone RVSB2-D (~7 – 0.8k cal a BP) (Figure 7). The lowest TOC amounts are observed in zones RVSB2-B, RVSB2-C and the region of the core devoid of pollen (~30 – 16k cal a BP). Short periods of low TOC are also seen between 5.0 – 4.1k cal a BP and 0.7 – 0.4k cal a BP. TN follows a similar trend to TOC and ranges between 0.02 and 2.06% (Figure 7). The pyrolysis data indicate relatively poor preservation of organic matter 16 – 30k cal a BP and 6 – 1.5k cal a BP (Figure 7), with much higher productivity and/or preservation inferred from 14k cal a BP, 9 – 6k cal a BP (which includes the increased preservation of lignin-derived pyrolysis products, perhaps indicative of more anaerobic conditions than preceding and subsequent periods; Carr et al., 2010) and during the last 1.5k cal a BP.

In general, $\delta^{13}C_{TOC}$ is fairly constant at c. -22‰ (which is more enriched than the pure C_3 vegetation; ~-27‰ (O'Leary, 1981)) except for clear excursions to lower values (-25‰ to -28‰) at 8.8 – 6.5k cal a BP, at 2.1 – 1.2k cal a BP and within zone RVSB2-A (Figure 7). The TOC/TN ratio is relatively constant for the upper 200 cm of the core, and fluctuates around an average of 16. The lower section is characterised by greater variability with values ranging from 6.7 to 58.2 (Figure 7). TOC/TN values rise steadily from the top of zone RVSB2-C to zone RVSB2-A. Apart from four data points (246 cm/11.2k cal a BP, 120 cm/4.5k cal a BP, 6 cm/ 0.05k cal a BP and 4 cm/0.02k cal a BP), all TOC/TN values are greater than 10, indicating that the organic matter within the core is largely derived from vascular plants (Meyers, 1994; Lamb et al., 2006).

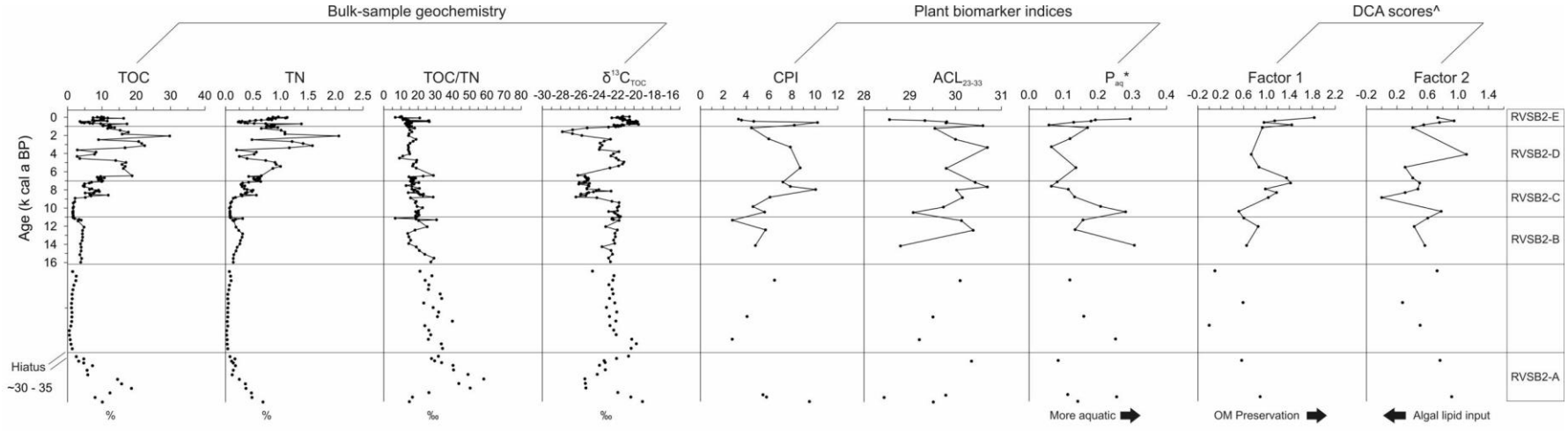
Bulk-sample geochemistry
Plant biomarker indices
DCA scores^
TOC
TN
TOC/TN
δ13CTOC
CPI
ACL23-33
Paq*
Factor 1
Factor 2
Age (k cal a BP)
RVSB2-E
RVSB2-D
RVSB2-C
RVSB2-B
RVSB2-A
Hiatus
~30 - 35
%
%
‰
‰
More aquatic
OM Preservation
Algal lipid input

Figure 7 *A plot of the RVSB-2 bulk-sample geochemical results (total organic carbon (TOC), total elemental nitrogen (TN), the ratio TOC/TN and* $\delta^{13}C$*), compound-specific isotopes (*$\delta^{13}C_{alkane}$ *and the proportion non-*C_3 *inputs) and selected plant biomarker indices: Carbon preference index (CPI,* C_{25}*–*C_{33}*, Equation 1). Average chain length (ACL, Equation 2) and* P_{aq} *(Equation 3) *Ficken et al. (2000). ^ Detrended correspondence analysis factor 1 and 2 scores from Carr et al. (2010). The zonation is based on the pollen record.*

4.4 Leaf wax lipids

The apolar lipid extracts are dominated by series of homologous *n*-alkanes spanning the chain length range C_{23} - C_{33}. Concentrations are generally low, and range between 2.2 and 0.1 μg g^{-1} (dry weight). *n*-alkane concentrations are positively correlated with TOC. The *n*-alkane distributions display a characteristic odd over even chain length preference, which is typically indicative of a higher plant origin (Eglinton and Hamilton, 1967; Pancost and Boot, 2004). The average chain length (ACL_{23-33}) of the extracted *n*-alkanes ranges from 28 – 31 carbon atoms (Figure 7), reflecting the dominance of the C_{29} and C_{31} *n*-alkanes in the majority of samples. This is consistent with a higher plant origin and is within the range of modern fynbos vegetation (Carr et al., 2014). ACL_{23-33} shows considerable down core variability, although with the exception of the most recent sample (22 cm) and the basal sample (360 cm), the C_{31} is always the dominant *n*-alkane. The proportion of shorter chain length (C_{23}-C_{25}) homologues is the major cause of this ACL_{23-33} variation. This variability is characterised by the 'P_{aq}' index (Ficken et al., 2000), which was proposed to be indicative of the contribution of non-emergent aquatic macrophytes relative to emergent aquatic and terrestrial plants. The P_{aq} is therefore commonly used to represent changes in aquatic plant inputs to organic matter within sedimentary sequences. Overall, the P_{aq} index is low throughout the record and is indicative of dominantly terrestrial or riparian vegetation inputs throughout the sequence. This is however consistent with the TOC/TN data and the py-GC/MS data. The highest P_{aq} (and shortest ACL_{23-33}) values are seen at c. 14k cal a BP, 11-8k cal a BP (RVSB2-C) and during the last 1k cal a BP (RVSB2-E). Relatively low values are observed throughout RVSB2-D, where the C_{29} and C_{31} n-alkanes are the dominant leaf waxes. The ratio of these two homologues is largely constant throughout the late glacial and the majority of the Holocene, with the exception of the last 1000 years. The ratio C31/(C31+C29) averages 0.67 ± 0.04 from 16 - 1k cal a BP (i.e. pollen zones RVSB2-B to RVSB2-D).

5 DISCUSSION

5.1 Depositional environment

The most marked feature of the sedimentary organic matter record is the clear reduction in OM quantity (TOC) and quality (DCA axis 1) between 30 and 16k cal a BP, at which point we also see an absence of preserved pollen. It is therefore likely that the site was seasonally or even permanently dry for periods of time within MIS 2. After 16k cal a BP, we observe consistent OM preservation. The pyrolysis data suggest periods with increased input of algal lipids and increased wetland productivity (notably 9 – 6k cal a BP; DCA axis 2, Figure 7), but overall the TOC/TN data (> 10 throughout) and the P_{aq} data suggest that the majority of sedimentary organic matter is terrestrial (vascular plant) in origin, and at no stage was the wetland a truly aquatic environment. The preservation of relatively labile organic matter components (notably cellulose and lignin) is generally poor throughout the record, with the exception of the most recent sediments and the period 9 – 6k cal a BP (Carr et al. 2010), suggesting oxic conditions, which would have been required in particular for the rapid microbially-mediated breakdown of macromolecule OM (Bourdon et al., 2000; Carr et al., 2010). The period 9 – 6k cal a BP is associated with a substantial increase in the abundance of algal lipids and prist-1-ene and prist-2-ene; the latter show particularly clear peaks within this period (data not shown) and were interpreted as pyrolysis products of chlorophyll - further evidence of enhanced primary production in the wetland (Carr et al. 2010). Together the bulk parameters, py-GC/MS dataset and the leaf wax data imply that although Rietvlei was never dominated by fully aquatic vegetation, the early Holocene (11 – 7k cal a BP), middle to late Holocene and last 1000 years stand out as geochemically distinct. The early and latest Holocene are likely associated with the most productive wetland conditions, and more humid climatic conditions overall, while the middle to late Holocene seemingly associated with a less productive wetland in which OM preservation was more restricted.

Taken at face value, the $\delta^{13}C_{TOC}$ data (Figure 7) emphasize the site's position within a transitional area encompassing fynbos, renonsterveld, coastal thicket/strandveld and karroid elements (Vogel et al., 1978; Cowling, 1983), but such regional-scale interpretations must be tempered by the undoubtedly large (and variable) contribution of local wetland vegetation to the sedimentary organic matter (Carr et al., 2015). With the exception of three negative excursions, $\delta^{13}C_{TOC}$ is relatively constant (-22 ‰). The most sustained excursion occurs

between 9 – 6k cal a BP (-26 ‰), a period of inferred enhanced productivity. This shift in $\delta^{13}C$ was hypothesized to reflect increased delivery of allochontonous organic matter from the fynbos-dominated vegetation surrounding the wetland during periods of increased humidity (Carr et al. 2010). In light of the now-available pollen data (specifically the strong coincident peaks in Proteaceae), the original interpretation by Carr et al. (2010) is supported. The higher resolution $\delta^{13}C_{TOC}$ (Figure **7**) record now available also indicated that a very similar situation (albeit shorter in duration) occurred immediately prior to 1k cal a BP and that variability of this nature may also have occurred during late MIS 3 (although the dating resolution for this section of the record is not sufficient to make more detailed observations).

Figure 8 *Comparison of selected Rietvlei-Still Bay variables and regional proxy evidence: A Iron concentrations from the Chilean continental margin at 41°C (Lamy et al., 2001); B Sea salt sodium concentrations from the EPICA DML ice core in Antarctica (Fischer et al., 2007); C The sum of the fynbos pollen taxa percentages in the Rietvlei-Still Bay core; D The Rietvlei-Still Bay* $\delta^{13}C$ *record; E Microscopic charcoal concentrations from the Rietvlei-Still Bay core; F The sum of succulent and/or drought-resistant pollen taxa percentages in the Rietvlei-Still Bay record; G The sum of afrotemperate forest and coastal thicket taxa percentages in the Rietvlei-Still Bay record; H The sum of aquatic and riparian pollen taxa percentages in the Rietvlei-Still Bay record; I Detrended correspondence analysis factor 1 scores from Carr et al. (2010); J Detrended correspondence analysis factor 2 scores from Carr et al. (2010); K Sea surface temperature (SST) stack from the precursor/upstream region of the Agulhas Current (marine core MD962048) (Caley et al., 2011b); L The* $\delta^{15}N$ *record from the Seweweekspoort-1-5 hyrax midden (Chase et al., 2013).*

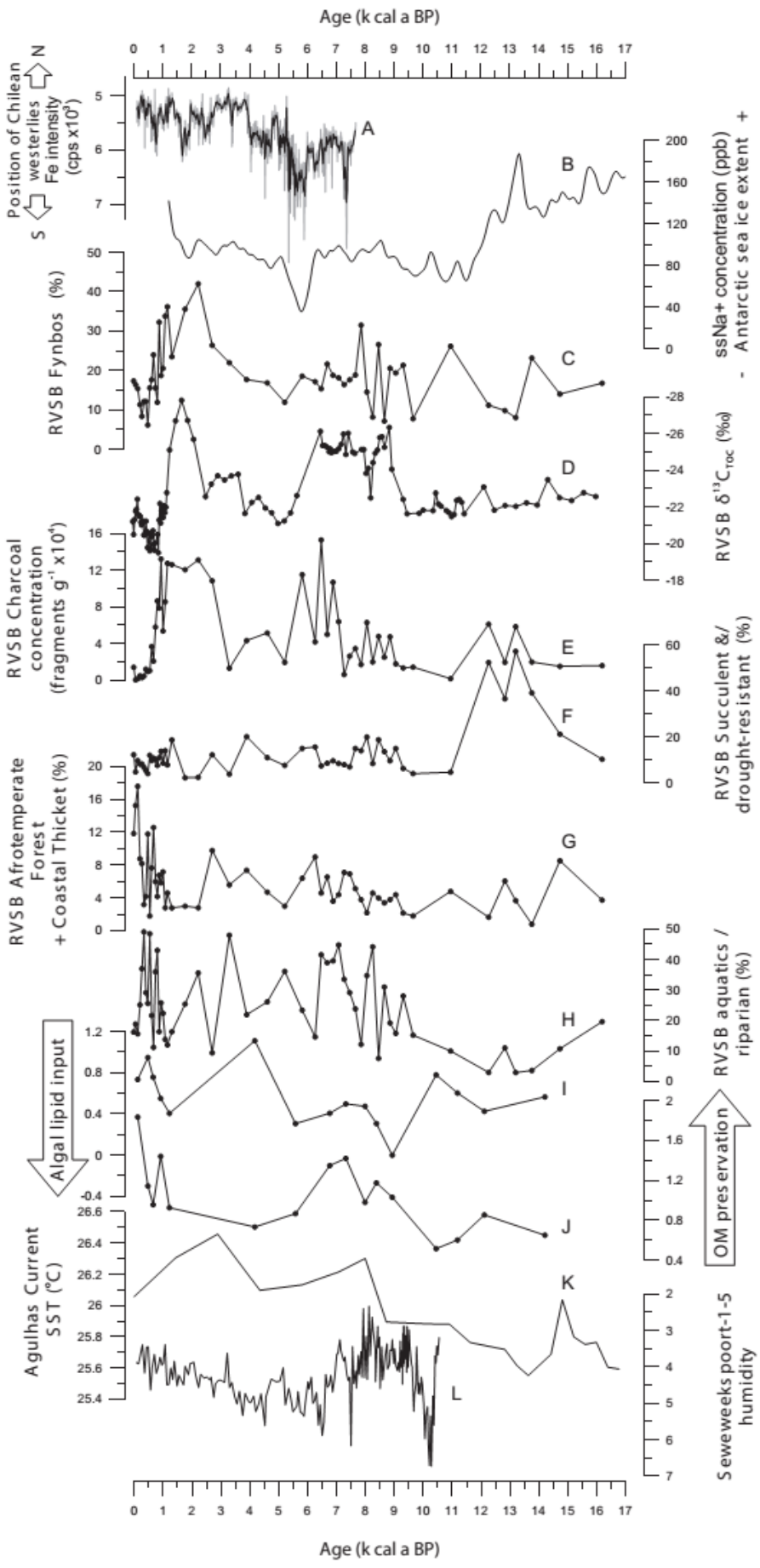
Age (k cal a BP)
Position of Chilean westerlies Fe intensity (cps x10³)
S
N
A
B
ssNa+ concentration (ppb)
- Antarctic sea ice extent +
RVSB Fynbos (%)
C
RVSB δ¹³C_TOC (‰)
D
RVSB Charcoal concentration (fragments g⁻¹ x10⁴)
E
RVSB Succulent &/ drought-resistant (%)
F
RVSB Afrotemperate Forest + Coastal Thicket (%)
G
H
Algal lipid input
RVSB aquatics / riparian (%)
I
OM preservation
J
Agulhas Current SST (°C)
K
L
Seweweeks poort-1-5 humidity
Age (k cal a BP)

523

5.2 Palaeoenvironmental change at Rietvlei-Still Bay

The Rietvlei sequence encompasses a period of time within which marked changes in regional palaeoenvironments are thought to have taken place, albeit with specific details and timings often poorly resolved (see Chase and Meadows, 2007). The multi-proxy record from Rietvlei provides a first detailed archive of such changes for the southern Cape coastal lowlands. Given the climatic setting of this region, the nature and timing of these changes have important implications for the overall southern Cape year round/winter rainfall zone, and thus regional hemispheric palaeoclimatic conditions.

5.2.1 MIS 3 (~35 – 30k cal a BP)

The geochemical, palynological and biomarker evidence indicates that, although wetland conditions prevailed at the site, the system was not very productive. For this section, two issues should be kept in mind: 1) it was not possible to construct a reliable age-depth model with the available data, and the unit should be considered as a snapshot of conditions in the ~35 – 30k cal a BP period, and 2) sea-level at this time was substantially lower than present (-80 m as per Waelbroeck et al., 2002), which would have resulted in a lower water table. Wetland development at the site would have thus relied much more heavily on direct rainfall than it would have after ~9 – 7k cal a BP (Carr et al., 2006a; Carr et al., 2006b). This latter point is particularly relevant when considering the fossil assemblage, wherein the presence of *Pseudoschizaea* shells/spores within sediments could in some instances indicate local seasonal drying (Scott, 1992). Indeed, the combination of increased succulents and/drought resistant taxa, the very prominent peak in *Pseudoschizaea* (Figure 5), moderate axis 1 and 2 pyrolysis DCA scores and low P_{aq} suggests a more ephemeral wetland during this period. Vegetation surrounding the vlei included a greater proportion of succulents, drought resistant shrubs and cosmopolitan shrubs such as *Anthospermum* and *Artemisia*, probably indicating relatively cool conditions under a seasonal rainfall regime. Under these cooler conditions, low percentages of fynbos pollen, with the exception of Restionaceae, and elevated xeric taxa may reflect drier conditions. Limited tree and tall shrub elements may reflect elevated drought stress and/or a more intense fire regime, as indicated by the high charcoal concentrations. Notable environmental variation within this 30-35k cal a BP period is however apparent; near the top of this unit, lower $\delta^{13}C_{TOC}$ values and relatively high TOC in

555 conjunction with increased percentages of aquatics and/ riparian pollen suggests increased
556 wetland productivity and better OM preservation.

557 Little reliable information is available regarding southern Cape palaeoenvironments
558 during MIS 3. The evidence that does exist suggests conditions were cooler and more humid
559 than today (Schalke, 1973; Avery, 1982; Klein, 1983; Deacon et al., 1984; Klein, 1984; Klein
560 et al., 1999; Scott et al., 2004; Carr et al., 2006b). These conditions could perhaps be related
561 to enhanced winter rainfall, wherein northward shifts in the STF (Peeters et al., 2004) may
562 have resulted in an equatorward shift of the westerly storm track (Stuut et al., 2002; Chase,
563 2010). The Rietvlei data suggest a less productive wetland than the present, although whether
564 this was a function of more arid environments or a lower water table cannot be fully resolved.
565 Given this and the chronological uncertainties, the data from Rietvlei are not necessarily
566 inconsistent with previously reported evidence for more humid MIS 3 conditions on the
567 southern Cape.

568 *5.2.2 Late MIS 3 to late MIS 2 (~30 – 16k cal a BP)*

569 Limited wetland productivity is inferred from the presence of highly degraded OM (Carr et
570 al., 2010) and the lack of pollen preservation during this period. Further evidence for
571 desiccation of the wetland environment is seen in the oxidation (slight orange mottling) of the
572 sediments within this section which imply shallow-water conditions or sub-aerial exposure
573 (Carr et al., 2010), probably under relatively drier conditions compared with the ~35-30k cal
574 a BP period.

575 While high southern latitude climate dynamics appear to have resulted in more humid
576 conditions in the WRZ, they may have had the opposite effect on the south coast (Meadows
577 and Baxter, 1999; Chase and Meadows, 2007). Significantly lower sea levels during the LGM
578 would have resulted in an extended coastal plain that may have altered local atmospheric
579 dynamics to the extent that an enhanced and/or expanded continental anticyclone blocked the
580 penetration of winter rainfall systems to the southern Cape (Cowling et al., 1999; Carr et al.,
581 2006b). Furthermore, decreased Agulhas Current SSTs would have led to decreased
582 advection of moisture over the adjacent coastal areas, in turn resulting in the reduced
583 incidence of moisture-bearing systems such as cut-off lows and ridging anticyclones, which
584 are responsible for a large portion of present-day rainfall. Therefore, despite potential
585 increases in winter rainfall in the WRZ, these factors together with reduced summer rainfall

and a potentially markedly lower water table at this time (Carr et al. 2006a) may have resulted in increased seasonality and overall drier conditions in the southern Cape.

5.2.3 Last glacial-interglacial transition (~16 – 11k cal a BP)

The last glacial-interglacial transition (LGIT) is evident in the core lithology by an increase in OM preservation. The RVSB-2 pollen record recommences at 16k cal a BP with increased percentages of fynbos and wetland taxa. Fynbos at the site reflects substantial winter rainfall and/or generally cool temperatures, as indicated by regional palaeotemperature reconstructions (Heaton et al., 1986; Talma and Vogel, 1992; Truc et al., 2013). This was followed rapidly by a phase of relatively dry conditions and/or warmer temperatures (e.g. reduced fynbos, low aquatic/riparian taxa percentages, high percentages of *ChenoAm*-type pollen and peaks in charcoal) between 14.8 and 11k cal a BP (Figure 8). This corresponds closely to a phase of lunette dune accumulation at Voëlvlei (presently a perennial lake) on the Agulhas Plain, 200 km to the west (Carr et al., 2006a; Figure 2). The decline in fynbos pollen after ~16 k cal a BP may be related to the warming evidenced at Pakhuis Pass, in the Cederberg Mountains of the Western Cape (Scott and Woodborne, 2007b, a), with both sites responding to the build-up of heat in the southern oceans as a response to reductions in Atlantic Meridional Overturning Circulation (AMOC) during Heinrich stadial 1 (Broecker, 1998; Stocker, 1998; Stocker and Johnsen, 2003).

5.2.4 The Holocene (~11 – 0k cal a BP)

For the early Holocene, ~11 – 9k cal a BP, TOC remains relatively low, but the py-GC/MS data suggest steadily improving OM preservation and after ~9k cal a BP, major changes in the environment at the site are evident from every measured proxy. Most notable is the significantly enhanced wetland productivity, as indicated by substantial increases in TOC, overall OM preservation and greater proportions of algal-derived organic matter (DCA axis 2). This is particularly associated with the period 9-6k cal a BP, which is characterised by a prominent phase of lower $\delta^{13}C_{TOC}$, accompanied by elevated aquatic/riparian pollen (Figure 8). This period of greater productivity and likely permanent inundation (implied by the OM preservation) is the most distinct phase of the geochemical record and implies a substantial shift in the status of the wetland. It is, however, important to consider these changes in the context of regionally rising sea-levels. Regional evidence indicates increased marine influences and high mid-Holocene sea-levels at estuarine sites in the Western Cape (Compton, 2001; Carr et al., 2015) and southern Cape (Reddering, 1988) from ~8.5-4k cal a BP. As elsewhere along the coast, this transgression would have raised the water table at

Rietvlei (Carr et al., 2006a; Carr et al., 2006b) and potentially contributed to the establishment of a more permanent wetland. Sea-level changes during the early Holocene, while not negligible, are generally thought to have been on the order of 1-3 meters (Compton, 2001; Bateman et al., 2004) and their impact on the Rietvlei record during the Holocene is likely to have been less significant than during the late Pleistocene.

Within the context of the Holocene sequence, pollen evidence suggests the period ~11 to 9k cal a BP was generally cool (elevated fynbos pollen), but variable, and relatively mesic and/or less seasonal (low percentages of succulent-drought resistant taxa and charcoal concentrations). From 9 – 8k cal a BP, increases in both succulent-drought resistant taxa and charcoal concentrations indicate slightly less and/or more seasonal precipitation, but apparent contradictions exist within the aggregate dataset. Proteaceae pollen is relatively abundant during this period, coincident with the reduction in $\delta^{13}C_{TOC}$ (Figure 8), and geochemical proxies suggest a perennial wet and productive wetland. Evidence from Elands Bay Cave in the southwestern Cape (Klein and Cruz-Uribe, 1987; Klein, 1991; Parkington et al., 2000) indicates that this may be a transitional period, with progressively drier conditions being attributed to a decline in winter rainfall (Chase and Meadows, 2007), and the evidence from Rietvlei may be reflecting – with lags and sensitivities specific to individual proxies – a transition from a cool, wet early Holocene to warmer and drier mid-Holocene climates (Chase and Meadows, 2007).

The period from 6-2k cal a BP shows distinct changes in pollen composition, with notable reductions in Proteaceae, some of the aquatic/riparian pollen types, *ChenoAm*-type and, towards the top of the zone, Poaceae. Charcoal peaks between 7-5k cal a BP and then becomes less abundant until 2k cal a BP, while OM preservation is relatively poor, and $\delta^{13}C$ is relatively high for the Holocene. Elsewhere, after ~7k cal a BP, evidence for drier conditions have been inferred from across the region, including Elands Bay Cave (Klein and Cruz-Uribe, 1987; Klein, 1991; Parkington et al., 2000), Klaarfontein (Meadows and Baxter, 2001), Cecilia Cave (Baxter, 1989), and Pakhuis Pass (Scott and Woodborne, 2007b, a) in the west, and Boomplaas Cave (Scholtz, 1986), Norga (Scholtz, 1986), Groenvlei (Martin, 1968) and Vankervelsvlei (Irving, 1998) in the south. Recent high resolution stable isotope records obtained from rock hyrax middens from Seweweekspoort (Chase et al., 2012; Chase et al., 2013) better constrain this period of relative aridity as a significant anomaly occurring between 7.0-5.0k cal a BP, and being linked to reductions in Antarctic sea-ice extent (Fischer et al., 2007) and the position of the westerly storm track (Lamy et al., 2001)(Figure 8). Data from Rietvlei-Still Bay (e.g. prominent charcoal peaks between 7.0 – 5.5k cal a BP and

reduced OM preservation) also suggest that the mid-Holocene was characterised by warmer and drier conditions. Some sites at the transition between winter and aseasonal rainfall zones, such as Katbakkies Pass (Meadows et al., 2010; Chase et al., 2015) and Byneskranskop (Avery, 1993), have provided evidence indicating increases in summer, and generally more mesic conditions during the middle Holocene, but at Rietvlei such increases in humidity are not clear from the data available.

The late Holocene at Rietvlei begins with a period of relatively low charcoal concentrations from 5.0-3.3k cal a BP, reduced fynbos abundance, and an increase in afrotemperate and thicket pollen, which may correspond to the phase of renewed forest development at Norga (Scholtz, 1986), and more humid conditions at Seweweekspoort (Chase et al., 2013), an equatorward shift of the westerlies (Lamy et al., 2001), and generally more mesic conditions with reduced rainfall seasonality (Chase and Meadows, 2007). In contrast, between ~3-1k cal a BP, a strong increase in charcoal concentrations is observed at Rietvlei. This coincides with slightly drier conditions at Seweweekspoort, indications for a poleward shift of the westerlies, drier conditions at Norga and phases of lunette accumulation at Voëlvlei and Buffelsjacht Pan (2.8-2.5 ka and 1.25 ka) on the Agulhas Plain (Carr et al., 2006b). A strong fynbos presence during this latter period may suggest that conditions were generally cool, probably still with significant winter rainfall, but increased rainfall seasonality may have elevated fire frequencies and promoted the development fynbos taxa over fire-prone afrotemperate and thicket elements (Figure 8). It is worth noting that these findings differ from interpretations of the pollen record from Princess Vlei, on the Cape Peninsula (Neumann et al., 2011). Incorporating refinements on the published linear age model using *Bacon* (version 2.2) (Blaauw and Christen, 2011), the period of wetter conditions inferred from changes in Factor 2 of the authors' principal components analysis, occurs between 3.5k – 2.1k cal a BP. Whether the opposing trends reflect local conditions, and/or distinct sensitivities to factors such as sea-level change remain to be more explicitly explored.

In the last thousand years, charcoal concentrations and fynbos pollen percentages decrease significantly (Figure 8). Succulent and drought-resistant taxa also become less abundant, and in accord with evidence at Norga for forest expansion (Scholtz, 1986), afrotemperate forest taxa increase markedly in the RVSB2 record. The substantial increases in Cyperaceae and Poaceae during that last 1k cal a BP are perhaps indicative of the development of the contemporary floating vegetation mat, a process that seemingly occurs in conjunction with increased abundances of several aquatic pollen types and increased P_{aq}/lower ACL/lower CPI. Combined, these suggest a shift to a more advanced hydroseral

phase in response to increased moisture availability and perhaps a more aseasonal rainfall regime. The decline in fynbos taxa is inconsistent with inferences of increased winter rainfall in the southwestern Cape over the last 1500 years based on diatom data from Verlorenvlei (Stager et al., 2012). This may be due to the spatial complexity of the southwestern Cape or it may be that increased summer rainfall during this period resulted in more mesic conditions, which suppressed fire frequencies and favoured the expansion of afrotemperate and thicket taxa at the expense of fynbos.

6 CONCLUSIONS

We present a multi-proxy record derived from the Rietvlei-Still Bay wetland, which reveals that considerable palaeoenvironmental change has taken place along the southern Cape coast during the late Pleistocene and Holocene. The results of the pollen analysis suggest that there were significant vegetation community reorganisations within this important region of the Fynbos Biome/CFR. Fynbos was particularly dominant within the late glacial period (~16k cal a BP), the early Holocene (~11 – 8k cal a BP) and from 2.2 – 0.9k cal a BP and its presence shows some commonalities with the relative influence of the westerly systems, as recently reported in other high resolution records. Succulent/drought resistant and more cosmopolitan elements characterised the MIS 3 section (~35 – 30k cal a BP) as well as the mid Holocene (6.9 – 3.3k cal a BP), while coastal thicket and afrotemperate forest were the dominant vegetation types for the most recent period (0.9 – 0k cal a BP).

Inferences from the vegetation dynamics, together with the geochemical and plant biomarker data, indicate that there were substantial changes in wetland productivity and overall moisture availability at the site. Interestingly, the stable carbon isotope ($\delta^{13}C_{TOC}$) record reveals long periods of stability punctuated by short episodes of marked reductions that correspond closely to shifts in the abundance of fynbos pollen and charcoal abundance. The Rietvlei wetland was relatively less productive than present during MIS 3 (~35 - 30k cal a BP) either as a function of more arid conditions and/or due to a lower water table. Drier and/ warmer conditions prevailed between 16 – 11.7k cal a BP and for much of the period 7 – 3.3k cal a BP. Relatively more humid and/ cooler conditions together with enhanced winter rainfall were associated with the early Holocene (11.7 – 7k cal a BP) and the phase 2.2 – 0.9k cal a BP. The establishment of a more aseasonal rainfall regime coupled with warmer temperatures took place from 0.9k cal a BP to present.

Being influenced by a variety of factors including rainfall amount and seasonality, atmospheric and oceanic temperatures, atmospheric CO_2, sea levels and ocean currents, the southern Cape coast's climatic and vegetation histories are complex. Despite this, several aspects of the RVSB record are consistent with the regional palaeoenvironmental record and suggest that the relative dominance of different moisture-bearing systems have greatly influenced the region.

Acknowledgements

LJQ acknowledges the financial assistance of the National Research Foundation (NRF) of South Africa, PAST (Palaeontological Scientific Trust) and the University of Cape Town. ASC was supported by the Quaternary Research Association and the University of Leicester. AB, ASC, MEM and BMC's contributions were supported by the European Research Council (ERC) under the European Union's Seventh Framework Programme (FP7/2007-2013)/ERC Starting Grant "HYRAX", grant agreement no. 258657 and the Leverhulme Trust (Grant F/00 212/AF). We thank Mr Guy Gardener for access to the Rietvlei wetland.

REFERENCES

Aitken MJ. 1985. *Thermoluminescence Dating*. Academic Press: London and New York.

Avery DM. 1982. Micromammals as palaeoenvironmental indicators and an interpretation of the late Quaternary in the southern Cape Province, South Africa. *Annals of the South African Museum* **85**: 183-377.

Avery DM. 1993. Last Interglacial and Holocene Altithermal environments in South Africa and Namibia: micromammalian evidence. *Palaeogeography, Palaeoclimatology, Palaeoecology* **101**: 221-228.

Bard E, Rickaby REM. 2009. Migration of the subtropical front as a modulator of glacial climate. *Nature* **460**: 380-383.

Bateman MD, Catt JA. 1996. An absolute chronology for the raised beach and associated deposits at Sewerby, East Yorkshire, England. *Journal of Quaternary Science* **11**: 389-395.

Bateman MD, Holmes PJ, Carr AS, Horton BP, Jaiswal MK. 2004. Aeolianite and barrier dune construction spanning the last two glacial-interglacial cycles from the southern Cape coast, South Africa. *Quaternary Science Reviews* **23**: 1681-1698.

Baxter A. 1989. *Pollen analysis of a Table Mountain cave deposit*. Unpublished BSc (Hons) Thesis, University of Cape Town: Cape Town.

Baxter A. 1996. *Late Quaternary Palaeoenvironments of the Sandveld, Western Cape Province, South Africa*. Unpublished PhD Thesis, University of Cape Town: Cape Town.

Blaauw M, Christen JA. 2011. Flexible paleoclimate age-depth models using an autoregressive gamma process. *Bayesian Analysis* **6**: 457-474.

Bourdon S, Laggoun-Défarge F, Disnar J-R, Maman O, Guillet B, Derenne S, Largeau C. 2000. Organic matter sources and early diagenetic degradation in a tropical peaty marsh

(Tritrivakely, Madagascar). Implications for environmental reconstruction during the Sub-Atlantic. *Organic Geochemistry* **31**: 421-438.
Bray EE, Evans ED. 1961. Distribution of n -paraffins as a clue to recognition of source beds. *Geochimica et Cosmochimica Acta* **22**: 2-15.
Broecker WS. 1998. Paleocean circulation during the last deglaciation: a bipolar seesaw? *Paleoceanography* **13**: 119-121.
Caley T, Kim JH, Malaizé B, Giraudeau J, Laepple T, Caillon N, Charlier K, Rebaubier H, Rossignol L, Castañeda IS, Schouten S, Sinninghe Damsté JS. 2011a. High-latitude obliquity as a dominant forcing in the Agulhas current system. *Climates of the Past* **7**: 1285-1296.
Caley T, Kim JH, Malaizé B, Giraudeau J, Laepple T, Caillon N, Charlier K, Rebaubier H, Rossignol L, Castañeda IS, Schouten S, Sinninghe Damsté JS. 2011b. High-latitude obliquity as a dominant forcing in the Agulhas current system. *Clim. Past* **7**: 1285-1296.
Carr A, Boom A, Chase B, Roberts D, Roberts Z. 2010. Molecular fingerprinting of wetland organic matter using pyrolysis-GC/MS: an example from the southern Cape coastline of South Africa. *Journal of Paleolimnology* **44**: 947-961.
Carr AS, Boom A, Chase BM, Meadows ME, Grimes HL. 2015. Holocene sea level and environmental change on the west coast of South Africa: evidence from plant biomarkers, stable isotopes and pollen. *Journal of Paleolimnology* **53**: 415-432.
Carr AS, Boom A, Chase BM, Meadows ME, Roberts ZE, Britton MN, Cumming AMJ. 2013. Biome-scale characterisation and differentiation of semi-arid and arid zone soil organic matter compositions using pyrolysis–GC/MS analysis. *Geoderma* **200–201**: 189-201.
Carr AS, Boom A, Grimes HL, Chase BM, Meadows ME, Harris A. 2014. Leaf wax *n*-alkane distributions in arid zone South African flora: environmental controls, chemotaxonomy and palaeoecological implications. *Organic Geochemistry* **67**: 72-84.
Carr AS, Thomas DSG, Bateman MD. 2006a. Climatic and sea level controls on late Quaternary eolian activity on the Agulhas Plain, South Africa. *Quaternary Research* **65**: 252-263.
Carr AS, Thomas DSG, Bateman MD, Meadows ME, Chase B. 2006b. Late Quaternary palaeoenvironments of the winter-rainfall zone of southern Africa: palynological and sedimentological evidence from the Agulhas Plain. *Palaeogeography, Palaeoclimatology, Palaeoecology* **239**: 147-165.
Chase BM. 2010. South African palaeoenvironments during marine oxygen isotope stage 4: a context for the Howiesons Poort and Still Bay industries. *Journal of Archaeological Science* **37**: 1359-1366.
Chase BM, Boom A, Carr AS, Meadows ME, Reimer PJ. 2013. Holocene climate change in southernmost South Africa: rock hyrax middens record shifts in the southern westerlies. *Quaternary Science Reviews* **82**: 199-205.
Chase BM, Lim S, Chevalier M, Boom A, Carr AS, Meadows ME, Reimer PJ. 2015. Influence of tropical easterlies in southern Africa's winter rainfall zone during the Holocene. *Quaternary Science Reviews* **107**: 138-148.
Chase BM, Meadows ME. 2007. Late Quaternary dynamics of southern Africa's winter rainfall zone. *Earth-Science Reviews* **84**: 103-138.
Chase BM, Scott L, Meadows ME, Gil-Romera G, Boom A, Carr AS, Reimer PJ, Truc L, Valsecchi V, Quick LJ. 2012. Rock hyrax middens: a palaeoenvironmental archive for southern African drylands. *Quaternary Science Reviews* **56**: 107-125.
Climate Systems Analysis Group UCT. 2012. *Climate Information Portal (CIP).* http://cip.csag.uct.ac.za/webclient/map. Accessed on: 15 March 2012.
Cohen AL, Tyson PD. 1995. Sea surface temperature fluctuations during the Holocene off the south coast of Africa: implications for terrestrial climate and rainfall. *Holocene* **5**: 304-312.

Compton JS. 2001. Holocene sea-level fluctuations inferred from the evolution of depositional environments of the southern Langebaan Lagoon salt marsh, South Africa. *Holocene* **11**: 395-405.
Cowling RM. 1983. The occurrence of C3 and C4 grasses in fynbos and allied shrublands in the South Eastern Cape, South Africa. *Oecologia* **58**: 121-127.
Cowling RM, Cartwright CR, Parkington JE, Allsopp JC. 1999. Fossil wood charcoal assemblages from Elands Bay Cave, South Africa: implications for late Quaternary vegetation and climates in the winter-rainfall fynbos biome. *Journal of Biogeography* **26**: 367-378.
Cowling RM, Holmes PM. 1992. Endemism and speciation in a lowland flora from the Cape Floristic Region. *Biological Journal of the Linnean Society* **47**: 367-383.
Deacon HJ, Deacon J, Scholtz A, Thackeray JF, Brink JS. 1984. Correlation of palaeoenvironmental data from the Late Pleistocene and Holocene deposits at Boomplaas Cave, southern Cape. In: *Late Cainozoic Palaeoclimates of the Southern Hemisphere*, Vogel JC (Ed.). Balkema: Rotterdam; pp. 339-360.
Eglinton G, Hamilton RJ. 1967. Leaf Epicuticular Waxes. *Science* **156**: 1322-1335.
Faegri K, Iversen J. 1989. *Textbook of Pollen Analysis*, 4th ed. John Wiley & Sons: Chichester.
Ficken KJ, Li B, Swain DL, Eglinton G. 2000. An n-alkane proxy for the sedimentary input of submerged/floating freshwater aquatic macrophytes. *Organic Geochemistry* **31**: 745-749.
Fischer H, Fundel F, Ruth U, Twarloh B, Wegner A, Udisti R, Becagli S, Castellano E, Morganti A, Severi M, Wolff E, Littot G, Röthlisberger R, Mulvaney R, Hutterli MA, Kaufmann P, Federer U, Lambert F, Bigler M, Hansson M, Jonsell U, de Angelis M, Boutron C, Siggaard-Andersen M-L, Steffensen JP, Barbante C, Gaspari V, Gabrielli P, Wagenbach D. 2007. Reconstruction of millennial changes in dust emission, transport and regional sea ice coverage using the deep EPICA ice cores from the Atlantic and Indian Ocean sector of Antarctica. *Earth and Planetary Science Letters* **260**: 340-354.
Grimm E. 1987. Coniss: A fortran 77 program for stratigraphically constrained cluster analysis by the method of incremental sum of squares. *Computers and Geosciences* **13**: 13-35.
Hammer Ø, Harper DAT, Ryan PD. 2001. PAST: Paleontological statistics software package for education and data analysis. Palaeontologia Electronica 4(1): 9pp. http://palaeo-electronica.org/2001_1/past/issue1_01.htm.
Heaton THE, Talma AS, Vogel JC. 1986. Dissolved gas paleotemperatures and 18O variations derived from groundwater near Uitenhage, South Africa. *Quaternary Research* **25**: 79-88.
Hogg AG, Hua Q, Blackwell PG, Niu M, Buck CE, Guilderson TP, Heaton TJ, Palmer JG, Reimer PJ, Reimer RW. 2013. SHCal13 Southern Hemisphere Calibration, 0–50,000 cal yr BP. *Radiocarbon* **55**: 1889-1903.
Hua Q, Barbetti M, Rakowski AZ. 2013. Atmospheric Radiocarbon for the Period 1950–2010. *Radiocarbon* **55**: 2059 - 2072.
Irving SJE. 1998. *Late Quaternary palaeoenvironments at Vankervelsvlei, near Knysna, South Africa*. University of Cape Town: Cape Town.
Kaal J, Baldock JA, Buurman P, Nierop KGJ, Pontevedra-Pombal X, Martínez-Cortizas A. 2007. Evaluating pyrolysis–GC/MS and 13C CPMAS NMR in conjunction with a molecular mixing model of the Penido Vello peat deposit, NW Spain. *Organic Geochemistry* **38**: 1097-1111.
Klein RG. 1983. Palaeoenvironmental implications of Quaternary large mammals in the Fynbos region. In: *Fynbos Palaeoecology: a preliminary synthesis*, Deacon HJ, Hendey, Q.B. and Lambrechts, J.J.N. (Ed.), 75 ed; pp. 116-138.

Klein RG. 1984. The large animals of southern Africa: late Pliocene to recent. In: *Southern African Prehistory and Palaeoenvironments*, Klein RG (Ed.). Balkema: Rotterdam; pp. 107-146.
Klein RG. 1991. Size variation in the Cape dune molerat (*Bathyergus suillus*) and late Quaternary climatic change in the southwestern Cape Province, South Africa. *Quaternary Research* **36**: 243-256.
Klein RG, Cruz-Uribe K. 1987. Large mammal and tortoise bones from Elands Bay Cave and nearby sites, western Cape Province, South Africa. In: *Papers in the Prehistory of the Western Cape*, Parkington J, and Hall, M. (Ed.): Oxford; pp. 132-163.
Klein RG, Cruz-Uribe K, Halkett D, Hart T, Parkington JE. 1999. Paleoenvironmental and human behavioral implications of the Boegoeberg 1 Late Pleistocene hyena den, Northern Cape Province, South Africa. *Quaternary Research* **52**: 393-403.
Lamb AL, Wilson GP, Leng MJ. 2006. A review of coastal palaeoclimate and relative sea-level reconstructions using $\delta^{13}C$ and C/N ratios in organic material. *Earth-Science Reviews* **75**: 29-57.
Lamy F, Hebbeln D, Rohl U, Wefer G. 2001. Holocene rainfall variability in southern Chile: a marine record of latitudinal shifts of the Southern Westerlies. *Earth and Planetary Science Letters* **185**: 369-382.
Lanesky DE, Logan BW, Brown RG, Hine AC. 1979. A new approach to portable vibracoring underwater and on land. *Journal of Sedimentary Petrology* **49**: 654–657.
Martin ARH. 1968. Pollen analysis of Groenvlei lake sediments, Knysna (South Africa). *Review of Palaeobotany and Palynology* **7**: 107-144.
Meadows ME, Baxter AJ. 1999. Late Quaternary palaeoenvironments of the southwestern Cape, South Africa: a regional synthesis. *Quaternary International* **57-8**: 193-206.
Meadows ME, Baxter AJ. 2001. Holocene vegetation history and palaeoenvironments at Klaarfontein Springs, Western Cape, South Africa. *Holocene* **11**: 699-706.
Meadows ME, Chase BM, Seliane M. 2010. Holocene palaeoenvironments of the Cederberg and Swartruggens mountains, Western Cape, South Africa: Pollen and stable isotope evidence from hyrax dung middens. *Journal of Arid Environments* **74**: 786-793.
Meyers PA. 1994. Preservation of elemental and isotopic source identification of sedimentary organic matter. *Chemical Geology* **114**: 289-302.
Mooney SD, Tinner W. 2011. The analysis of charcoal in peat and organic sediments. *Mires and Peat* **7**: 1-18.
Moore PD, Webb JA, Collinson ME. 1991. *Pollen Analysis*, 2nd ed. Blackwell Scientific Publications: Oxford.
Mucina L, Rutherford MC. 2006. The vegetation of South Africa, Lesotho and Swaziland. In: *Strelitzia*. South African National Biodiversity Institute: Pretoria.
Mustart PJ, Cowling RM, Albertyn J. 2003. *Southern Overberg South African Wild Flower Guide 8*. Botanical Society of South Africa: Cape Town.
Nakagawa T, Brugiapaglia E, Digerfeldt G, Reille M, De Beaulieu J-L, Yasuda Y. 1998. Dense media separation as a more efficient pollen extraction method for use with organic sediment/deposit samples: comparison with the conventional method. *Boreas* **27**: 15-24.
Neumann FH, Scott L, Bamford MK. 2011. Climate change and human disturbance of fynbos vegetation during the late Holocene at Princess Vlei, Western Cape, South Africa. *The Holocene* **21**: 1137-1149.
Nierop KGJ. 1998. Origin of aliphatic compounds in a forest soil. *Organic Geochemistry* **29**: 1009-1016.
O'Leary MH. 1981. Carbon isotope fractionation in plants. *Phytochemistry* **20**: 553-567.
Pancost RD, Boot CS. 2004. The palaeoclimatic utility of terrestrial biomarkers in marine sediments. *Marine Chemistry* **92**: 239-261.

Parkington J, Cartwright C, Cowling RM, Baxter A, Meadows M. 2000. Palaeovegetation at the Last Glacial Maximum in the Western Cape, South Africa: wood charcoal and pollen evidence from Elands Bay Cave. *South African Journal of Science* **96**: 543-546.
Patterson WA, Edwards KJ, Maguire DJ. 1987. Microscopic charcoal as a fossil indicator of fire. *Quaternary Science Reviews* **6**: 3-23.
Peeters FJC, Acheson R, Brummer G-JA, de Ruijter WPM, Schneider RR, Ganssen GM, Ufkes E, Kroon D. 2004. Vigorous exchange between the Indian and Atlantic oceans at the end of the past five glacial periods. *Nature* **430**: 661-665.
Poynter JA, Farrimond P, Brassell SC, Eglinton G. 1989. Aeolian-derived higher plant lipids in the marine sedimentary record: links with paleoclimate
In: *Palaeoclimatology and palaeometeorology: modern and past patterns of global atmosphere transport*, Leinen M, Sarnthein M (Eds.). D. Kluwer: Dordrecht; pp. 435–462.
Prescott JR, Hutton JT. 1994. Cosmic ray contributions to dose rates for luminescence and ESR dating: large depths and long-term variations. *Radiation Measurements* **23**: 497-500.
Rebelo AG, Cowling RM, Campbell BM, Meadows ME. 1991. Plant communities of the Riversdale Plain. . *South African Journal of Botany* **57**: 10–28.
Reddering JSV. 1988. Evidence for a middle Holocene transgression, Keurbooms estuary, South Africa. *Palaeoecology of Africa* **19**: 79-86.
Roberts DL, Bateman MD, Murray-Wallace CV, Carr AS, Holmes PJ. 2008. Last Interglacial fossil elephant trackways dated by OSL/AAR in coastal aeolianites, Still Bay, South Africa. *Palaeogeography, Palaeoclimatology, Palaeoecology* **257**: 261-279.
Schalke HJWG. 1973. The Upper Quaternary of the Cape Flats area. *Scripta Geologica* **15**: 1-57.
Scholtz A. 1986. *Palynological and Palaeobotanical Studies in the Southern Cape*. University of Stellenbosch: Stellenbosch, South Africa.
Scott L. 1982. Late Quaternary fossil pollen grains from the Transvaal, South Africa. *Review of Palaeobotany and Palynology* **36**: 241-278.
Scott L, Marais E, Brook GA. 2004. Fossil hyrax dung and evidence of Late Pleistocene and Holocene vegetation types in the Namib Desert. *Journal of Quaternary Science* **19**: 829-832.
Scott L, Woodborne S. 2007a. Pollen analysis and dating of Late Quaternary faecal deposits (hyraceum) in the Cederberg, Western Cape, South Africa. *Review of Palaeobotany and Palynology* **144**: 123-134.
Scott L, Woodborne S. 2007b. Vegetation history inferred from pollen in Late Quaternary faecal deposits (hyraceum) in the Cape winter-rain region and its bearing on past climates in South Africa. *Quaternary Science Reviews* **26**: 941-953.
Stager JC, Mayewski PA, White J, Chase BM, Neumann FH, Meadows ME, King CD, Dixon DA. 2012. Precipitation variability in the winter rainfall zone of South Africa during the last 1400 yr linked to the austral westerlies. *Clim. Past* **8**: 877-887.
Stocker TF. 1998. The seesaw effect. *Science* **282**: 61-62.
Stocker TF, Johnsen SJ. 2003. A minimum thermodynamic model for the bipolar seesaw. *Paleoceanography* **18**.
Stockmarr J. 1973. Determination of spore concentration with an electronic particle counter. *Danmarks geologiske undersøgelse Arbog*: 87–89.
Stuiver M, Polach HA. 1977. Discussion: reporting of ^{14}C data. *Radiocarbon* **19**: 355-363.
Stuut J-BW, Prins MA, Schneider RR, Weltje GJ, Jansen JHF, Postma G. 2002. A 300 kyr record of aridity and wind strength in southwestern Africa: inferences from grain-size distributions of sediments on Walvis Ridge, SE Atlantic. *Marine Geology* **180**: 221-233.
Talma AS, Vogel JC. 1992. Late Quaternary paleotemperatures derived from a speleothem from Cango Caves, Cape Province, South Africa. *Quaternary Research* **37**: 203-213.

Truc L, Chevalier M, Favier C, Cheddadi R, Meadows ME, Scott L, Carr AS, Smith GF, Chase BM. 2013. Quantification of climate change for the last 20,000 years from Wonderkrater, South Africa: implications for the long-term dynamics of the Intertropical Convergence Zone. *Palaeogeography, Palaeoclimatology, Palaeoecology* **386**: 575-587.
van Zinderen Bakker EM. 1953. *South African pollen grains and spores. Volume I*. Balkema: Amsterdam–Cape Town.
van Zinderen Bakker EM. 1956. *South African pollen grains and spores. Volume II*. Balkema: Amsterdam–Cape Town.
van Zinderen Bakker EM, Coetzee JA. 1959. *South African pollen grains and spores. Volume III*. Balkema: Amsterdam–Cape Town.
Vancampenhout K, Wouters K, Caus A, Buurman P, Swennen R, Deckers J. 2008. Fingerprinting of soil organic matter as a proxy for assessing climate and vegetation changes in last interglacial palaeosols (Veldwezelt, Belgium). *Quaternary Research* **69**: 145-162.
Vogel JC, Fuls A, Ellis RP. 1978. The geographic distribution of Krantz species in southern Africa. *South African Journal of Science* **75**: 209-215.
Waelbroeck C, Labeyrie L, Michel E, Duplessy JC, McManus J, Lambeck K, Balbon E, Labracherie M. 2002. Sea-level and deep water temperature changes derived from benthic foraminifera isotopic records. *Quaternary Science Reviews* **21**: 295-305.
Welman WG, Kuhn L. 1970. *South African pollen grains and spores. Volume VI*. Balkema: Amsterdam–Cape Town.
Willis CK, Lombard AT, Cowling RM, Heydenrych BJ, Burgers CJ. 1996. Reserve systems for limestone endemic flora of the cape lowland fynbos: Iterative versus linear programming. *Biological Conservation* **77**: 53-62.

Table 1: Uncalibrated ages and calibration details for RVSB-2.

Lab code	Average depth (cm)	Measurement method	^{14}C age yr BP	F14C ± 1 σ	1 sigma error	Calibration data	95.4 % (2σ) cal BP age range	Relative area under distribution	Median probability	Date (2σ) range (AD)	OSL age (ka)	OSL age error (ka)
UBA-19735	2.5	AMS	Greater than modern^	1.0103 ± 0.0048		Southern Hemisphere Zone 1 and 2[#]				1955 - 1957		
A-14939	88.0	GPC	1260		70	SHCal13 †	977 – 1274	1	1133			
A-15438	133.0	GPC	5365		60	SHCal13 †	5942 – 5973 5984 – 6221 6232 – 6275	0.048 0.870 0.082	6103			
UBA-18048	207.5	AMS	8166		39	SHCal13 †	8990 – 9144 9169 - 9250	0.900 0.100	9067			
Shfd08157	224.5	OSL									11.27	0.6
A-14938	255.0	GPC	10250		120	SHCal13 †	11397 – 12319 12321 - 12404	0.946 0.054	11881			
UBA-19737	274.5	AMS	13439		58	SHCal13 †	15837 – 16246	1	16050			
UBA-19736	331.5	AMS	29496		264	SHCal13 †	33024 – 34094	1	34189			
A-14937	351.5	GPC	27630		1065	SHCal13 †	29546 – 33842	1	32280			

AMS = Accelerated mass spectrometry
GPC = Gas proportional counting
OSL = Optically stimulated luminescence
^Modern = 1950 AD
F14C = fraction modern
# Hua et al. (2013)
† Hogg et al. (2013)

FIGURE CAPTIONS:

Figure 1 The location of the southern Cape (black box) in relation to generalised atmospheric and oceanic circulation patterns. ABF: Angola-Benguela Front, CAB: Congo Air Boundary, ITCZ: Inter Tropical Convergence Zone.

Figure 2 A map showing the location of the Rietvlei wetland, the approximate positions of the winter rainfall (WRZ), year-round rainfall (YRZ) and summer rainfall (SRZ) zones, the biomes of South Africa (Mucina and Rutherford, 2006) and the published palaeoenvironmental and archaeological records within the region (A). 1 Elands Bay Cave, 2 Grootdrift, 3 Verlorenvlei, 4 Klaarfontein Springs, 5 Pakhuis Pass, 6 Sneeuberg Vlei and Driehoek Vlei, 7 De Rif, 8 Truitjes Kraal, 9 Katbakkies, 10 Rietvlei, 11 Cape Flats, 12 Princess Vlei, 13 Hangklip, 14 Die Kelders, 15 The Agulhas Plain vleis and lunettes (Soetendalsvlei, Voëlvlei, Renosterkop and Soutpan), 16 Blombos Cave, 17 Seweweekspoort 18 Pinnacle Point, 19 Norga peats, 20 Cango Cave and Boomplaas Cave, 21 Groenvlei, 22 Nelson Bay Cave and 23 Uitenhage Aquifer. The position of the coring site (RVSB-2) in relation to the wetland and local vegetation (Mucina and Rutherford, 2006) (B).

Figure 3 Stratigraphic description of the RVSB-2 core employing the Troel-Smith sediment notation.

Figure 4 The RVSB-2 age-depth model produced by the *Bacon* software package (Blaauw and Christen, 2011). ^{14}C ages were calibrated with the SHCal13 curve (Hogg, 2013) and the post-bomb age was calibrated with the Southern Hemisphere post-bomb curve by Hua et al. (2013). The median probability calibrated ages are labelled and the uncalibrated ages with errors are provided in parentheses (apart from the first age range which is the greater than modern sample's AD date range). The model is based on 19 15-cm thick sections of piece-wise linear accumulations, grey-scales indicate all likely age-depth models, grey dotted lines show the 95% confidence intervals and red curve shows single 'best' model based on the weighted mean age for each depth. Note the OSL date is not calibrated nor reported BP but for ease of plotting has been included on the same axis label.

Figure 5 Relative percentage pollen diagram for RVSB-2. Taxa are grouped according to general ecological affinities and are plotted against interpolated age (k cal a BP). Exaggeration curves are 5x and taxa representing less than 1% for any given level are presented as presence points. Non-pollen palynomorphs are represented as percentages of the total pollen count but not included in the count. Zonation is based on the results of a CONISS analysis.

Figure 6 Microscopic charcoal fragments per gram sample in the RVSB-2 core, illustrated for the two size classes and the total fragments. Charcoal concentration calculated in the same manner as pollen concentrations using *Lycopodium* spore counts. The zonation is based on the pollen record.

Figure 7 A plot of the RVSB-2 bulk-sample geochemical results (total organic carbon (TOC), total elemental nitrogen (TN), the ratio TOC/TN and $\delta^{13}C$), compound-specific isotopes ($\delta^{13}C_{alkane}$ and the proportion non-C_3 inputs) and selected plant biomarker indices: Carbon preference index (CPI, C_{25}–C_{33}, Equation 1). Average chain length (ACL, Equation 2) and P_{aq} (Equation 3) *Ficken et al. (2000). ^ Detrended correspondence analysis factor 1 and 2 scores from Carr et al. (2010). The zonation is based on the pollen record.

Figure 8 Comparison of selected Rietvlei-Still Bay variables and regional proxy evidence: A Iron concentrations from the Chilean continental margin at 41°C (Lamy et al., 2001); B Sea salt sodium concentrations from the EPICA DML ice core in Antarctica (Fischer et al., 2007); C The sum of the fynbos pollen taxa percentages in the Rietvlei-Still Bay core; D The Rietvlei-Still Bay $\delta^{13}C$ record; E Microscopic charcoal concentrations from the Rietvlei-Still Bay core; F The sum of succulent and/or drought-resistant pollen taxa percentages in the Rietvlei-Still Bay record; G The sum of afrotemperate forest and coastal thicket taxa percentages in the Rietvlei-Still Bay record; H The sum of aquatic and riparian pollen taxa percentages in the Rietvlei-Still Bay record; I Detrended correspondence analysis factor 1 scores from Carr et al. (2010); J Detrended correspondence analysis factor 2 scores from Carr et al. (2010); K Sea surface temperature (SST) stack from the precursor/upstream region of the Agulhas Current (marine core MD962048) (Caley et al., 2011b); L The $\delta^{15}N$ record from the Seweweekspoort-1-5 hyrax midden (Chase et al., 2013).